A11105 627726

NIST
PUBLICATIONS

NISTIR 6395

Transport Properties and Durability of Concrete: Literature Review and Research Plan

Dale P. Bentz
James R. Clifton
Chiara F. Ferraris
Edward J. Garboczi

Building and Fire Research Laboratory
Gaithersburg, Maryland 20899

NIST

QC
100
.U56
NO.6395
1999

ed States Department of Commerce
nology Administration
nal Institute of Standards and Technology

NISTIR 6395

Transport Properties and Durability of Concrete: Literature Review and Research Plan

Dale P. Bentz
James R. Clifton
Chiara F. Ferraris
Edward J. Garboczi

September 1999
Building and Fire Research Laboratory
National Institute of Standards and Technology
Gaithersburg, Maryland 20899

U.S. Department of Commerce
William M. Daley, *Secretary*
Technology Administration
Gary R. Bachula, *Under Secretary for Technology*
National Institute of Standards and Technology
Raymond G. Kammer, *Director*

ABSTRACT

The increased emphasis on life cycle cost analysis for building projects requires that new attention be focused on the service life and durability of concrete structures. While concrete is typically specified based on compressive strength and slump, it is well recognized that durability is most influenced by the transport properties of the concrete such as diffusivity, permeability, and sorptivity. This report reviews the state-of-the-art for measurement of transport properties in the laboratory and field and discusses the linkages between transport properties and models for various deterioration processes of relevance to highway concretes. Based on this review, a preliminary research approach and testing guidelines are presented for evaluating the durability of new and existing concretes for pavements. A key feature of the overall approach will be the development of a general model relating concrete sorptivity to spalling damage for three common degradation phenomena: sulfate attack, alkali-silica reaction, and freeze/thaw scaling.

Keywords: Building technology, concrete, durability, moisture content, pavement, permeability, service life, sorptivity, transport.

Contents

Abstract iii

List of Figures vii

1 Introduction 1

2 Theory of Transport 1
- 2.1 Sorption . . . 2
- 2.2 Gas Permeability . . . 3
- 2.3 Liquid Permeability . . . 4

3 Concrete Microstructure Considerations 5

4 Laboratory Test Methods 8
- 4.1 Sorption . . . 8
- 4.2 Gas Permeability . . . 9
- 4.3 Liquid Permeability . . . 10
- 4.4 Specimen Pre-Conditioning . . . 11

5 Field Test Methods 12
- 5.1 Sorption . . . 12
- 5.2 Permeability . . . 14
- 5.3 RH and Moisture Content Assessment . . . 15

6 Relationships Between Transport and Durability 16
- 6.1 Carbonation . . . 16
- 6.2 Sulfate Attack . . . 17
- 6.3 Alkali-Silica Reaction . . . 18
- 6.4 Freeze/Thaw Damage . . . 19
- 6.5 Acid Attack and Leaching . . . 20

7 Recommended Approach 21

8 Conclusions 23

9 Notation 24

10 Useful Constants 26

11 Acknowledgements 26

12 References 26

A Example Calculation of Service Life of Concrete Exposed to Sulfate Attack 34

B Proposed Testing Guidelines **35**
B.1 Pre-Conditioning 35
B.2 Sorptivity 36
B.3 Gas Permeability 39

List of Figures

1 Spatial variation in aggregate density for a simulated volume of concrete 30 × 30 × 60) mm in size at a magnification of 2x [33]. Brightness indicates the concentration of aggregate at each (x,y) location in the image. The dark quarter circle in upper right is one quarter of a rebar and the cast surface is at the left edge of the image. 6

2 Simulated aggregate distribution in concrete as a function of distance from the cast surface for a 3-D system with rebar centered at a depth of 60 mm [33]. 7

3 Basic experimental setup for laboratory evaluation of concrete sorptivity. . . 8

4 Basic experimental setup for laboratory evaluation of concrete gas permeability. 9

5 Basic experimental setup for ISAT evaluation of concrete sorptivity onsite. . 13

6 Flowchart illustrating proposed experimental protocol. 22

7 Basic NIST setup for laboratory evaluation of concrete sorptivity. 38

8 Basic NIST setup for laboratory evaluation of concrete gas permeability. . . 41

1 Introduction

The durability of concrete has become a worldwide concern during the latter part of the 20th century. Many of the structures built in the 1960's and 1970's have seriously deteriorated and substantial funding is now needed for maintenance and repair, in addition to new construction. The situation is compounded by the fact that concrete technology has changed significantly in the last 20 years. The introduction of high-strength and high-performance concretes has resulted in substantial changes in the mixture proportioning from the practices employed in the 1970's. These new-generation concretes are expected to provide significant increases in service lifetimes, but a methodology to ensure durability performance is still lacking. The specification of compressive strength alone is insufficient to guarantee the durability of a concrete [1, 2, 3]. Among other reasons, the durability of a concrete is greatly influenced by the properties of the surface and near-surface layers, while compressive strength is more of a bulk property. Additionally, strength is controlled by flaw (pore) size while transport is typically dominated by the overall connectivity (percolation) of the pore network. Thus, to adequately ensure the durability of a concrete, properties other than compressive strength must be specified [4]. The interaction of the surface layer of the concrete with the immediate external environment is of paramount importance in many degradation processes (ingress of chlorides and sulfates, carbonation, wetting/drying cycles). For this reason, an evaluation of the transport properties of this surface layer should provide a valuable indication of the durability of a given concrete.

Relevant transport properties include ionic diffusion, gas diffusion, liquid sorption, gas permeability, and liquid permeability. Because the Federal Highway Administration has funded other research projects which focus on ionic diffusion in concrete, the NIST study will be limited to consideration of the sorption and permeability properties of the concrete. Much research has been conducted on the development of laboratory and field tests for evaluating these properties, but the direct linkage of these properties to degradation models is much less developed. Despite this, durability indicators based on specific transport properties have been proposed for the cases of sorption [5, 6], carbonation [7, 8, 9], and frost damage [8]. This report will review the state-of-the-art and present a research approach for developing standard tests and guidelines for assessing the durability of field concrete.

While this report focuses on the concrete side of the concrete-environment interface, it is recognized that adequate and accurate characterization of the exposure environment is critical for performing realistic predictions of in-situ service life. As pointed out by Alexander and Ballim [10], durability studies require three main considerations: 1) complete and proper definition of the environment, 2) characterization of the material in the form of appropriate index values, and 3) test methods to ensure that the requisite index values have been met. While this study focuses on the latter two of these topics, the need for an integrated approach is well recognized by the authors.

2 Theory of Transport

The theory of transport in concrete has been reviewed by numerous authors [4, 11, 12, 13]. Here, we will focus on the basic equations that have relevance to the actual test methods employed in the laboratory and the field.

2.1 Sorption

The pores in concrete cover a wide range of sizes from nanometers to micrometers. When these pores come into contact with a wetting liquid phase, the liquid will invade due to the capillary forces present in each pore. The local capillary force is inversely proportional to the pore diameter, with smaller pores exerting a larger capillary force (although the rate of ingress into a smaller pore will actually be less than that into a larger one). For the case of one-dimensional flow, sorption of concrete is generally defined by its sorptivity, S, determined using the following equation [12]:

$$M(t) = \rho A S \sqrt{t} \tag{1}$$

where $M(t)$ represents the mass of liquid gained by the specimen at time t, ρ is the density of the invading liquid, A is the surface area of the specimen exposed to the liquid, and S is the sorptivity in units of length/time$^{0.5}$. For field concrete, the square-root-of-time dependency may not always be followed, as the exponent in the power law function may vary between 0.2 and 0.5 [14]. As an alternative to measuring mass gain, the depth of the liquid invasion front is sometimes assessed (by destructively breaking open the sample and directly observing the front). In this case, the governing equation is [15]:

$$d(t) = B \sqrt{t} \tag{2}$$

where d is the depth of liquid penetration after time t and B is the penetration coefficient [16]. Dividing S by B provides an estimate of the effective porosity of the concrete. In cases where the penetrating liquid front is difficult to identify, thermal imaging can be used to easily isolate the portion of the concrete undergoing evaporation, as the heat of vaporization results in a temperature drop in the fluid-saturated portion of the concrete [16], so that the fluid-saturated regions will appear darker (cooler) in a thermal image.

In practice, it is often observed that there is a rapid initial absorption (wetting of the dry surface, etc.) so that equations 1 and 2 are modified to:

$$M(t) = M_0 + \rho A S \sqrt{t} \tag{3}$$

$$d(t) = d_0 + B \sqrt{t} \tag{4}$$

where M_0 and d_0 represent the initial mass gain and initial depth of penetration, respectively. To determine S or B, either mass gain or penetration depth is plotted against the square root of time, and the initial straight line portion of the curve is used to evaluate the slope, equivalent to S or B.

Deviations from the square-root-of-time behavior at longer times have been observed in numerous experiments and are generally attributed to interactions of water with the concrete [16]. Both Hall [17] and Martys and Ferraris [18] have proposed modifications to Equation 3 to account for these long time deviations. The equation of Hall has the form:

$$M(t) = M_0 + \rho A (S t^{1/2} - C_H t) \tag{5}$$

while that of Martys and Ferraris is:

$$M(t) = M_0 + \rho A \left[S_g t^{1/2} + C_M (1 - exp\left(\frac{-S t^{1/2}}{C_M} \right)) \right] \tag{6}$$

where C_H and C_M are constants obtained from fitting the experimental data, and S_g describes the sorptivity in the smaller pores or the effects of moisture diffusion [18].

Temperature influences sorptivity through its effects on the surface tension (σ) and the dynamic viscosity (η) of the invading fluid. Hall indicates that S should scale as $(\sigma/\eta)^{0.5}$ [11]. Using this scaling relationship, measurements made at different temperatures can be normalized to a common standard temperature for comparative purposes. While this scaling relationship holds well for the absorption of organic fluids by concrete, significant deviations from the theory are observed when water is used as the sorbing fluid [16]. This could be due to the changing solubility of calcium hydroxide with temperature and the complex interactions of water with the concrete matrix.

While the one-dimensional flow boundary conditions are easy to maintain in the laboratory by using core specimens, this geometry is difficult to maintain in field testing. Recently, however, Wilson et al. [19] have derived appropriate equations for describing the sorption of a concrete slab, a circular portion of whose surface is exposed to a liquid. In this case, the penetrating liquid front takes the shape of an expanding 3-D ellipsoid as opposed to a flat interface in the one-dimensional flow case. The equation for this case is [19]:

$$M(t) = \rho A(\sqrt{\frac{\pi}{3}} S t^{1/2} + \frac{7}{8\sqrt{3}} \frac{\pi^{3/2} S^3}{f^2 L^2} t^{3/2} + \frac{1}{\sqrt{3}} \frac{147}{128} \frac{\pi^{5/2} S^5}{f^4 L^4} t^{5/2}) \tag{7}$$

where f is the porosity of the concrete and L is the diameter of the circular wetting source.

2.2 Gas Permeability

To measure gas permeability in the most direct manner, a pressure gradient is applied across a concrete specimen and the flow rate at steady state is measured. With this setup, the gas permeability, k_g, is given by [20]:

$$k_g = \frac{2Qx\eta P_f}{A(P_1^2 - P_2^2)} \tag{8}$$

where P_1 and P_2 are the upstream and downstream pressures, respectively, Q is the volumetric flowrate in m^3/s, x is the specimen thickness in m, A is the area for flow in m^2, and k_g is the permeability coefficient in units of m^2. P_f corresponds to the pressure at which the flowrate is measured, either P_1 or P_2, depending on the experimental setup.

When comparing gas permeabilities to liquid permeabilities, it is necessary to correct for the slippage of the gas, commonly referred to as the Klinkenberg correction [21, 22]. By measuring the gas permeability under a variety of pressure gradients, the intrinsic permeability (at infinite pressure) can be derived by fitting the data to an equation of the form:

$$k_l = \frac{k_g}{1 + \frac{b}{P_m}} \tag{9}$$

where k_l is the intrinsic permeability, P_m is the mean pressure of the inlet and outlet streams ($(P_1 + P_2)/2$), and b is a constant for a given gas and a given concrete. Practically, a plot of k_g vs. $(1/P_m)$ should yield a straight line with intercept k_l.

For the case of a variable pressure at the inlet, Yssorche et al. have derived simplified and complete theories for obtaining the permeability based on monitoring the change in height of

water in a capillary tube acting as a manometer [23]. For the simplified theory, permeability is given by:

$$k = \frac{\eta s x}{\rho A g t} ln\left(\frac{h_0}{h}\right) \tag{10}$$

where h is the height of water in the capillary tube at time t, h_0 is the initial height, s is the cross sectional area of the capillary tube, and g is the acceleration due to gravity. The complete theory, which accounts for the compressibility of the air in the testing apparatus, can be found in reference [23]. The authors generally found that the values estimated by the simplified theory were about 25 % lower than those calculated based on the complete theory.

Ballim [24] derives a similar equation for a falling head permeameter where the decreasing pressure is directly monitored. Transformed to the notation used in this report, his equation has the form:

$$k = \frac{\omega V \eta x}{\rho R A T t} ln\left(\frac{P_0}{P}\right) \tag{11}$$

where ω is the molecular mass of the gas in kg/mole, T is absolute temperature in degrees K, R is the universal gas constant, V is the volume of air under pressure in m^3, and P_0 and P are the pressures at the beginning and end of the test of duration t respectively.

2.3 Liquid Permeability

For the case of liquid flowing through concrete under an applied pressure gradient, the governing equation for determining intrinsic permeability is [20]:

$$k_l = \frac{Q x \eta}{A(P_1 - P_2)} \tag{12}$$

where all terms are as previously defined.

Once again, for field use, it is difficult to maintain one-dimensional flow. For the case of an ellipsoidal flow field emanating from a cylindrical source in a hole drilled in the concrete, Meletiou et al. [25] have derived:

$$k_l = \frac{Q}{2\pi H_o P} \sinh^{-1}\left(\frac{H_o}{2r_h}\right) \tag{13}$$

where H_o is the length of the test section, r_h is the radius of the test hole, and P is the applied pressure head. This equation holds for the range of $r_h \leq H_o < 10r_h$, conditions which are always satisfied in the field test developed by Meletiou et al.

At times, the measured permeabilities are expressed in units of m/s instead of m^2. The general conversion between these two systems is [4]:

$$k(m^2) = \frac{k(m/s) \cdot \eta}{\rho \cdot g}. \tag{14}$$

For water at a temperature of 20 °C, $k(m/s)$ =9.75 $\times 10^6$ $k(m^2)$ [4].

3 Concrete Microstructure Considerations

The transport properties of a concrete are controlled by the characteristics of its pore network. Total porosity, pore size, pore connectivity, and pore saturation all influence the measured transport coefficients [26]. The pore structure of a concrete is complex, spanning six or more orders of magnitude [27]. Sorptivity and permeability, the main transport properties being considered in this study, are both influenced by pore size and pore connectivity, with the largest connected pores (connected to the water source in the case of sorptivity and connected across the flow path for permeability) providing the easiest path for transfer of liquids and gases. In ordinary portland cement concrete, the largest pores are typically contained in the interfacial transition zones present between cement and aggregates [28]. Conversely, in high-performance concrete, these interfacial transition zones are practically eliminated and in some cases virtually no capillary porosity exists, so that transport is controlled by flow through the nanometer-sized pores present in the calcium silicate hydrate (*C–S–H*) gel [29]. Recent research indicates that the porosity of this gel is reduced when its formation is via the pozzolanic reaction of calcium hydroxide with silica fume (or fly ash) instead of via conventional hydration of the tricalcium and dicalcium silicate in the cement [30]. This will result in a further reduction in the transport coefficients of high-performance concrete containing pozzolans relative to conventional concrete. This all implies that high-performance and conventional concrete are quite different materials with respect to their pore structure, and care must be taken (in pre-conditioning, etc.) when measuring their transport properties for comparison purposes.

At equilibrium, the saturation of a concrete is determined by the pore structure and the local relative humidity (*RH*). Many of the pores in concrete are sufficiently small such that condensation will occur at *RH* values much less than 100 %. The relationship between the smallest pore radius with water condensate, r_p, and *RH* (for $RH > 40\%$) is described by the Kelvin-Laplace equation [27]:

$$ln(\frac{RH}{100}) = -\frac{2V_m\sigma}{r_pRT} \tag{15}$$

where V_m is the molar volume of water, and all other terms have been previously defined. The validity of this equation for $RH \leq 40\%$ is questionable due to both the capillary stress exceeding the tensile strength of water and the fact that the water meniscus would be composed of only about ten molecules. Equation 15 implies that, for two materials with the same porosity, the one with the larger pores will contain less condensed water at a specific *RH*. Because of the large range of pore sizes in concrete, there exists considerable hysteresis in the adsorption/desorption curves, due to ink-bottle and pore topology effects. Thus, simply knowing the *RH* of a concrete is insufficient for making an accurate estimate of its moisture content [29]. For this reason, the appropriate pre-conditioning of specimens presents an experimental difficulty. Fortunately, the desorption isotherms of many concretes are relatively flat in the range of 40 % to 80 % *RH*. so that pre-conditioning (from a saturated state) in an environmental chamber at about 60 % *RH* may be a viable option prior to gas permeability or sorptivity measurements provided that the concrete has not previously experienced substantially lower *RH* values in the field. Since the desorption isotherm is flat in this range, the saturation of the concrete will only vary slightly with the specific *RH* achieved in the interior of the concrete specimen. Recently, Abbas et al. [22] have shown that, within the saturation range of 20 % to 80 %, the logarithm of the gas

permeability is linearly proportional to the degree of saturation. Because the pore structure of concrete changes substantially at elevated temperatures [31] or when dried under vacuum [32], any oven drying should be performed at temperatures as low as possible which still allow equilibrium to be achieved in a reasonable time. Specific pre-conditioning regimes will be discussed later in the laboratory test method section of this report.

A further source of heterogeneity in concrete is the microstructural gradient which exists near a cast concrete surface. When a concrete is placed in the field, the cast surface will typically consist of a layer rich in cement paste, containing a lower fraction of aggregates [33]. Generally, a higher cement content results in a reduced resistance to transport [34], so that the surface layer indeed will often be the weak link with respect to durability. Figure 1 provides a view of the spatial variation in a simulated concrete slab. The lack of aggregate particles at the cast surface and near to the rebar can be easily observed. A quantitative analysis of this effect is provided in Fig. 2 which shows the variation in aggregate volume fraction as a function of distance from the cast concrete surface. Because of this spatial variability, the sorptivity and permeability properties of the first 5 mm to 10 mm away from a cast surface of a concrete may be quite different from those of the next 5 mm to 10 mm. When assessing transport properties for predicting durability, care must be taken to evaluate both the surface and near-surface concrete layers for an accurate assessment of overall performance. For this reason, the experimental approach recommended later in this report will include evaluation of the variability of concrete transport properties as a function of depth from the surface.

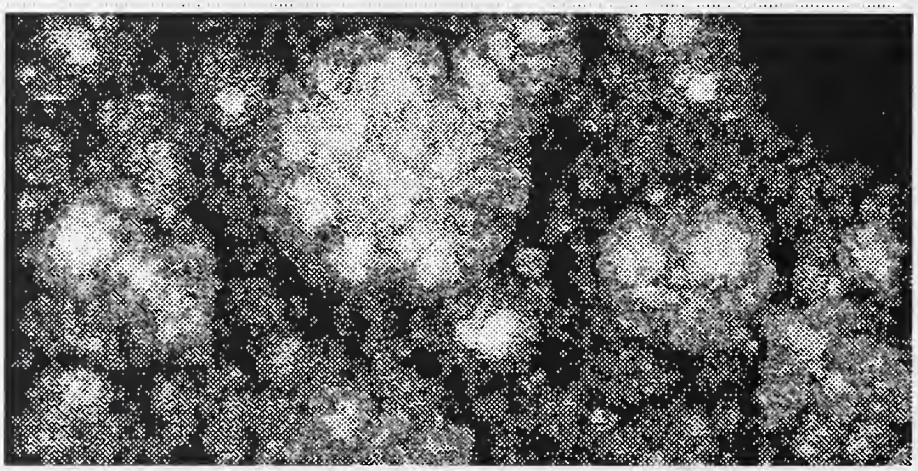

Figure 1: Spatial variation in aggregate density for a simulated volume of concrete 30 $\times$ 30 $\times$ 60) mm in size at a magnification of 2x [33]. Brightness indicates the concentration of aggregate at each (x,y) location in the image. The dark quarter circle in upper right is one quarter of a rebar and the cast surface is at the left edge of the image.

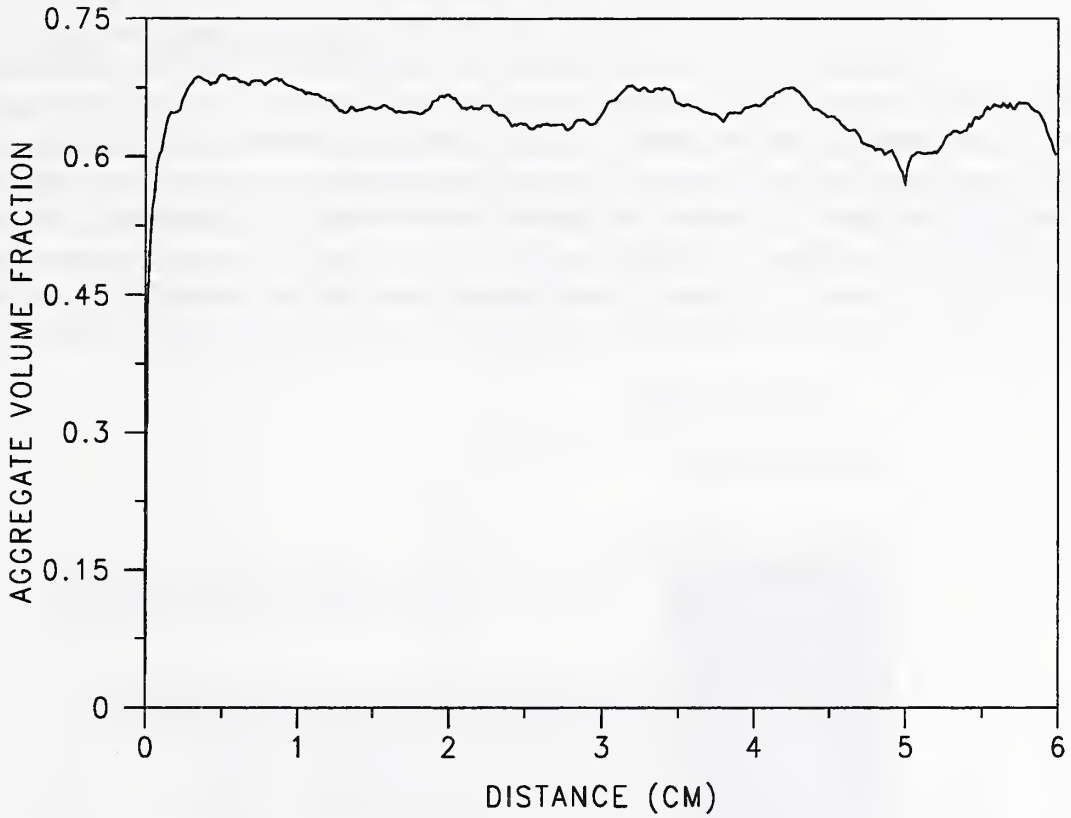

Figure 2: Simulated aggregate distribution in concrete as a function of distance from the cast surface for a 3-D system with rebar centered at a depth of 60 mm [33].

4 Laboratory Test Methods

4.1 Sorption

The basic setup for measuring water sorptivity in the laboratory is presented in Fig. 3 [18]. One face of a concrete specimen is placed in contact with water and its mass gain with time is monitored. To avoid evaporative effects, the remaining faces of the specimen are usually sealed using an epoxy resin or a tape. In the Swedish version of this test, the specimen is not sealed but the entire test is performed in a sealed box to eliminate evaporation effects [35], generally resulting in increased sorptivities values due to vapor diffusion and adsorption at the specimen surfaces not in contact with the water [36]. In the setup shown in Fig. 3, gravitational and capillary forces are in opposition, as opposed to the case when water is placed on top of the specimen where gravity and the capillary forces act cooperatively [16]. Because of the magnitude of the capillary forces present in mortars and concretes, water absorption rates measured with gravity in opposition, gravity in cooperation, or the effects of gravity totally removed (horizontal infiltration) are often indistinguishable [11]. To avoid excessive leaching of calcium hydroxide from the concrete during the test, some reseachers recommend using saturated calcium hydroxide solution as the sorbing fluid [16, 37], while others have noted little or no difference between this solution and ordinary distilled water [18].

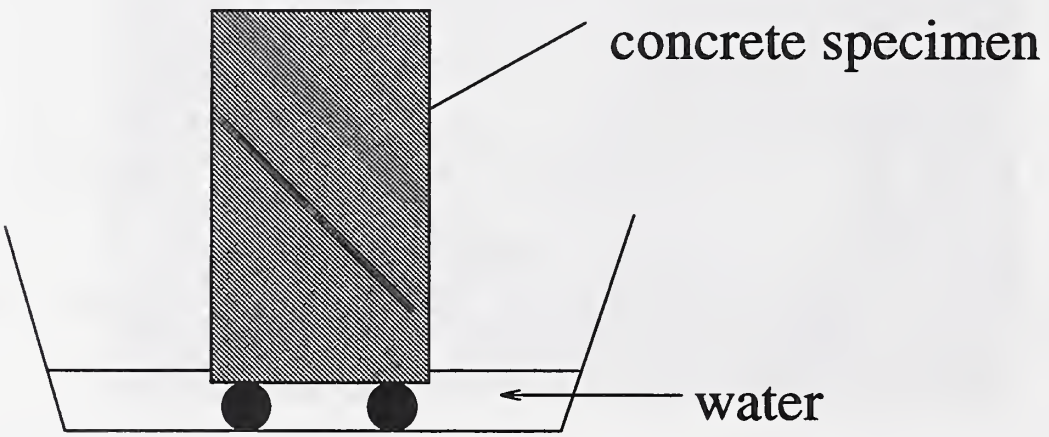

Figure 3: Basic experimental setup for laboratory evaluation of concrete sorptivity.

Variants of this test include placing water on top of the specimen as opposed to underneath it [16, 38], immersing the sealed specimen in water [39], using an absorbent paper at the specimen-water interface [37], using a water spray at a fixed pressure as the water source [15], and suspending the test specimen from an analytical balance so that its mass may be continuously monitored [39, 40]. The thickness (in the direction of the flow) of tested specimens varies: 15 mm [37, 40]; 50 mm [39, 41]; 60 mm [15]; and 100 mm [18]. From a

practical viewpoint, thicker specimens will take a much longer time to equilibrate with any pre-conditioning environment as the drying time should be proportional to the thickness squared if the drying process is diffusion controlled. Since the sorption occurs from the exposed surface, little advantage is obtained from using a thicker specimen if the concrete is of relatively sound quality such that the water front only penetrates a few millimeters during the first 4 h to 8 h of testing. Additionally, McCarter [42] has studied the influence of surface finish on measured sorptivity, finding considerably higher sorptivities for top (trowelled) than for bottom (cast) or cut surfaces. However, the measured depths of penetration, d, for the three specimens were similar, indicating that the increased sorptivity of the top surface is due mainly to its increased porosity, perhaps due to a higher paste content near the surface, or to inadequate curing of the surface concrete.

4.2 Gas Permeability

The usual experimental setup for measuring gas permeability of concrete in the laboratory is shown in Fig. 4. The concrete specimen (usually cylindrical) is sealed between two stainless steel plates, connected to a gas source (air or nitrogen). A pressure regulator is used to set the inlet pressure at the desired value, with the outlet pressure being atmospheric. A gas flowmeter in the downstream flow path is used to monitor the gas flow rate so that Equation 8 may be used to evaluate the permeability.

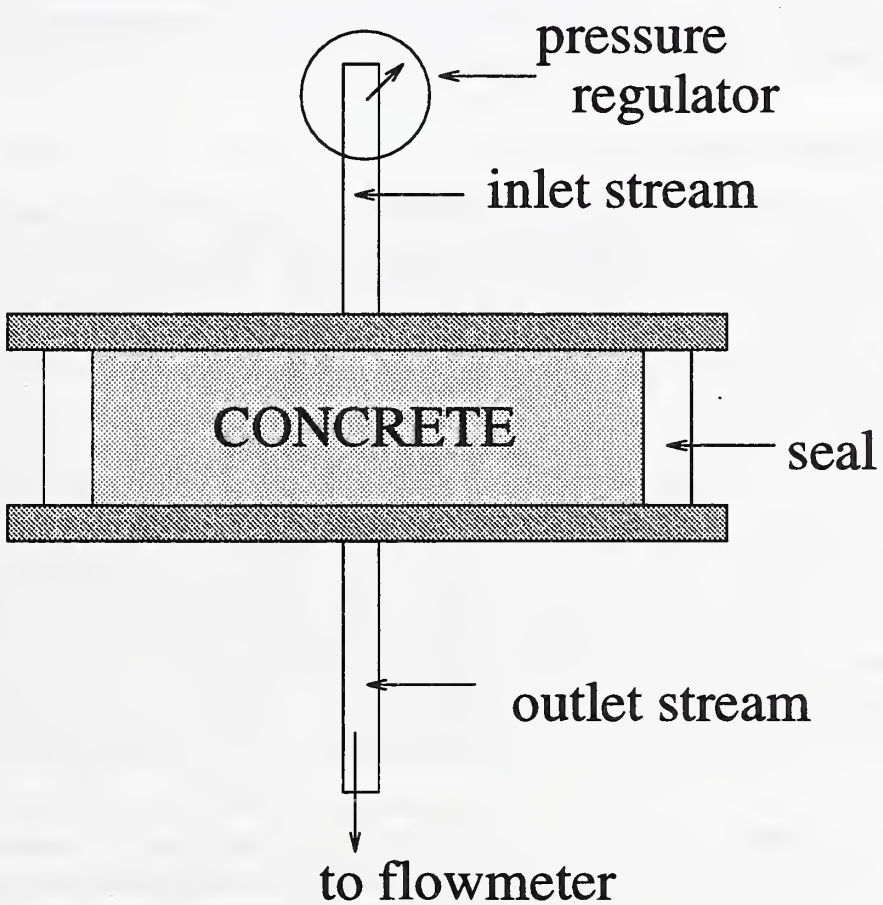

Figure 4: Basic experimental setup for laboratory evaluation of concrete gas permeability.

In the configuration shown in Fig. 4, if the seal is cast for each specimen, the specimen

thickness can be easily varied. Typical thicknesses are between 25 mm and 60 mm [43]. Pressure may be applied to the two end plates to achieve a tighter seal and prevent gas leakage [43]. To further prevent leakage, the curved side of the cylindrical specimen may be sealed using an epoxy resin [20]. A detailed description of a laboratory method for determining oxygen permeability has been developed by Cembureau [44]. Specimen preparation, equipment specification, and testing procedures are all discussed in this method.

Variations to this general method include passing the pressurized gas through a central hole in concrete cubes [45] or using a test setup in which the inlet [24] or outlet [23] pressure is allowed to vary over time. In the latter two cases, the flowrate is not monitored and permeability is instead calculated using Equation 10 or 11. In all cases, results are strongly influenced by the moisture content of the specimen, so that a standard pre-conditioning regime is a necessity if results from various laboratories are to be compared.

Schonlin and Hilsdorf [46] describe an interesting variant of the method shown in Fig. 4 in which the bottom plate is removed and the top inlet stream is attached to a vacuum pump. A rubber ring around the sample is used to seal it to the top plate via the vacuum pressure. The vacuum pressure decay over time is monitored and a transport coefficient is then determined using:

$$K = \frac{(P_1 - P_0)V_s x}{(t_1 - t_0)(P_{atm} - \frac{P_0+P_1}{2})A} \tag{16}$$

where P_0 and P_1 are the pressure inside the vacuum chamber at times t_0 and t_1, respectively, V_s is the volume of the vacuum chamber, P_{atm} is atmospheric pressure, and K is an arbitrary transport coefficient in units of m^2/s.

4.3 Liquid Permeability

The basic setup for measuring liquid permeability is similar to that for gas permeability shown in Fig. 4. In fact, several researchers have used essentially the same laboratory equipment for measuring both water and gas permeabilities [20, 43]. Generally, higher pressures are required to force the liquid through a saturated concrete. In addition, Hearn and Mills [43] recommend that both the inlet and outlet flow rates be monitored to assess steady state conditions, due to the numerous possible interactions between the water and the concrete specimen. Bamforth [20] alternatively suggests the measurement of penetration depth of the liquid as a function of time and subsequent calculation of a permeability coefficient. However, in this case, the heterogeneity of the concrete must be kept in mind when evaluating a specimen containing both a cast surface layer and bulk material, as the permeability characteristics of the surface layer are probably quite different from those of the bulk concrete within the same sample. For measuring liquid permeability, ideally, the specimen is completely saturated prior to testing to minimize the time required to reach a steady state. Still, for high performance concretes, weeks or months may be required to achieve a measurable cumulative flow in the downstream collection volume, even when starting from complete saturation.

Recently, a novel method for estimating the water permeability of cement-based materials has been developed by Scherer [47]. The method, first employed for evaluating the permeability of gels, is based on heating the specimen above ambient and monitoring the dimensional changes that occur with time. The length (for example) of the specimen will first increase to some local maximum, since the thermal expansion of water is greater than

that of the concrete. Because of the low concrete permeability, the water heats up well before any appreciable flow takes place. Therefore, at first, the water is essentially confined within the pores. As time progresses, the length will slowly decay to an equilibrium value determined by the thermal expansion coefficient of the solid backbone of the concrete. In this process, water is expelled from the specimen and the flowrate (or rate of decay of the length change) is indicative of the water permeability of the specimen. So far, this technique has only been preliminarily evaluated for cement pastes, but could be a promising solution for measuring the permeability of conventional concretes. Saturation of the specimen is still necessary, so there still may be limits on measuring the permeability of low permeability high-performance concretes using this technique.

4.4 Specimen Pre-Conditioning

Both sorptivities and permeabilities are strongly influenced by the water content of the concrete being evaluated [22]. As the water content is increased, more and more of the pores are filled with liquid water, which significantly alters both the sorption of liquid water and the transport of gas. Thus, even in laboratory testing, the pre-conditioning of the concrete specimens is of paramount importance. For comparison of different kinds of concrete, testing under a fixed set of laboratory conditions is desirable. If performance assessment in a specific environment is the goal, then testing under laboratory conditions that closely resemble those to be found in the field may be preferable.

For liquid permeabilities, the sample is first vacuum saturated. While straightforward for conventional concretes, for high performance concretes, complete saturation (even under a strong vacuum) can take a long time and may not be possible [20].

For sorptivity and gas permeability, many different pre-conditioning regimes have been employed to prepare the specimens for testing. Conventionally, drying at 105 °C has been the method of choice [3]. However, it is now well recognized that this preparation produces a moisture content that is atypical with respect to field conditions and results in elevated values for sorptivity and permeability coefficients [14]. The Cembureau method [44] recommends that one of the following two pre-conditioning regimes be employed: 1) storage in a laboratory atmosphere at 20 °C and 65 % RH for 28 days or 2) drying in a ventilated oven at 105 °C for 7 days followed by storage in a desiccator for 3 days at 20 °C. The French AFREM group has recommended oven drying at 80 °C with permeability measurements performed after 7 days and 28 days, but continues to evaluate alternative pre-conditioning regimes [49]. Following an extensive study, Parrott recommends drying in an oven at 50 °C for 3 days to 5 days, followed by sealed storage at 50 °C for 3 days to 5 days more to allow the moisture within the sample to equilibrate spatially [14], since mass equilibrium will not be reached during the initial few days. Following along this same research line, DeSouza et al. arrived at a recommendation of 3 days of 50 °C oven drying, followed by 4 days of sealed storage [41]. The sealed storage allows the moisture to spatially equilibrate within the sample, hopefully minimizing the gradient typically present after oven drying [49]. The total drying period of 7 days is reasonable and certainly more efficient than the 28 days required for method (1) of the Cembureau recommendation. This drying regime results in surface relative humidities greater than 40 % and total moisture contents greater than 1 % [41], conditions typical of many field concretes [48]. At these conditions, the capillary pores present in the concrete are generally empty, providing a pathway for the flow of air or the sorption of water. At relative humidities above 80 %, water will condense in these pores, and the measured gas

permeability and sorptivity will decrease markedly. For cement pastes, Galle et al. [50] have observed a decrease in gas permeability of five orders of magnitude (10^{-16} m^2 to 10^{-21} m^2) as *RH* varies from 10 % to 100 %, with values relatively constant between 40 % and 70 % *RH*.

At these intermediate relative humidities, carbonation is naturally a concern and appropriate precautions must be taken to limit the contact of the drying specimen with CO_2 environments. Thus, the samples should be kept in tightly sealed bags except during the actual testing time. Additionally, nitrogen, oxygen, or CO_2-free air should be used for the gas permeability testing.

5 Field Test Methods

5.1 Sorption

The first standardized test for measuring the sorption properties onsite was the Initial Surface Absorption Test (ISAT), described in detail by Levitt [51]. A schematic of the apparatus is shown in Fig. 5. Basically, a gasketed cap is sealed onto the concrete surface and the rate of water ingress from a reservoir supplying a pressure head of 200 mm is evaluated after 10 min, 30 min, 1 h, and 2 h. The attached capillary tube is used to measure the instantaneous flow rate at these specific times, with the reservoir valve being temporarily closed so that all the water going into the concrete is from the capillary source. The sorption is typically reported as $ml/m^2/s$. By numerically integrating the readings obtained at various times [52] a cumulative flow can be obtained and Equation 3 used to determine the concrete's sorptivity. This is of course an approximation, because the flow fields in this case are not one-dimensional [53], but rather ellipsoidal in nature. Price and Bamforth [52] have suggested the use of a water-filled guard ring to ensure one-dimensional ingress. Alternatively, the analytical equation of Wilson et al. [19], Equation 7, can be used to determine the sorptivity, provided that the cumulative volumetric ingress is monitored at times intermediate to those outlined in the basic ISAT procedure, to allow a more precise fit of the equation to the measured data.

An alternative to the ISAT, called the covercrete absorption test (CAT), has been proposed by Dhir et al. [54]. In this test, a test hole (13 mm in diameter by 50 mm deep) is first drilled in the site concrete and then the water sorption in the test hole measured in a manner similar to the ISAT measurement. Dhir et al. used this test on concrete cores that had been removed from field concrete and dried at 105 °C. Blight and Lampacher [55] have since applied the same test directly on field concrete (without oven drying). The "covercrete" absorption is reported in units of $ml/m^2/s$ and is not easily converted to a sorptivity, because of the complex flow invasion pattern from a cylindrical hole source (i.e., one-dimensional flow is definitely not maintained). An analysis similar to that developed by Meletiou et al. [25] for liquid permeability might be able to provide an equation relating sorptivity to flow measured in this experimental setup. In the authors' opinion, the ISAT test is more applicable since sorption will normally first occur from the top surface of the field concrete and not from its interior.

Attempts to further automate the ISAT test have been performed, and several systems are commercially available. Noble et al. [56] developed an automated system using a camera to monitor the meniscus in the capillary tube. Basheer et al. [57] have developed the

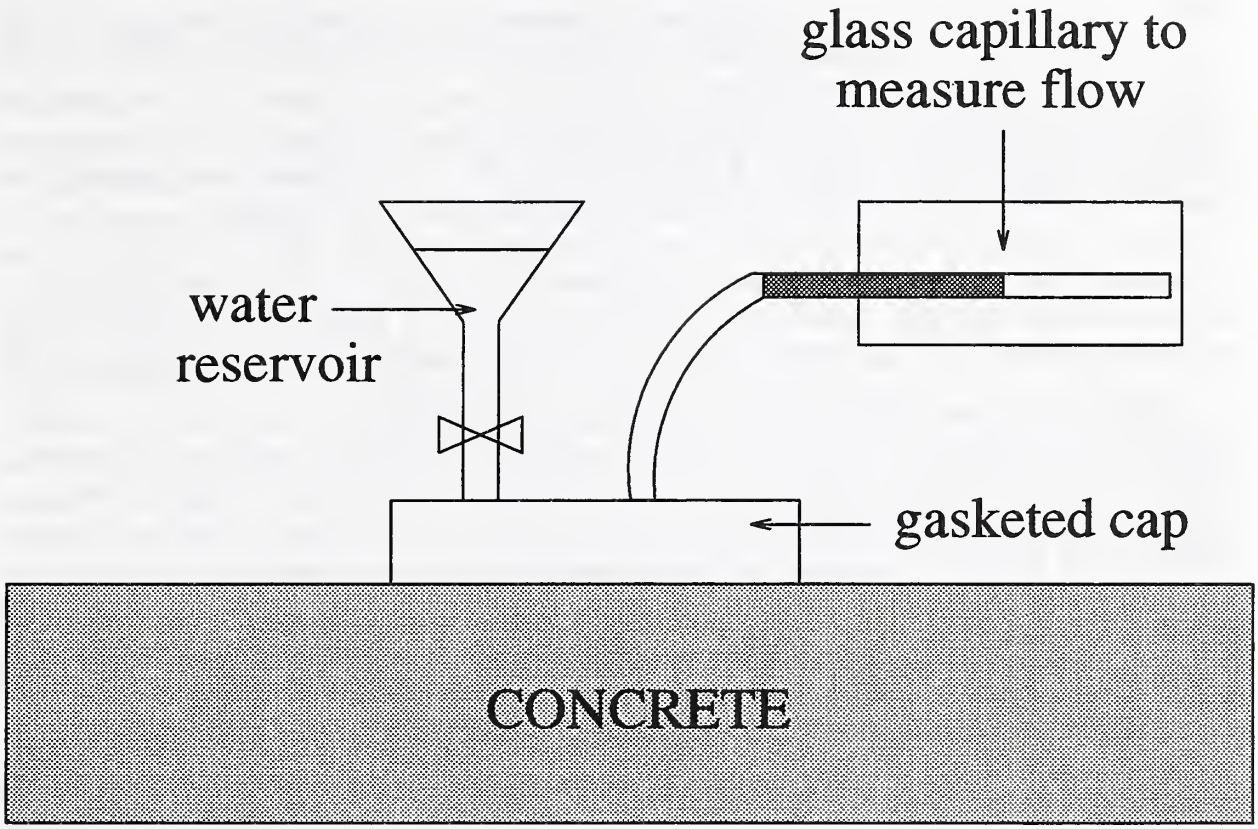

Figure 5: Basic experimental setup for ISAT evaluation of concrete sorptivity onsite.

"AutoClam" [1] for automatically assessing the permeation and sorption properties of concrete. Their apparatus is commercially available in the U.S. and throughout Europe. Sorptivity in $m^3/s^{0.5}$ is determined from the slope of a plot of cumulative water absorption vs. the square root of time. Because, once again, one-dimensional flow conditions are not maintained during the test, a better analysis could perhaps be obtained using the more complete equation 7 developed recently by Wilson et al. [19].

As in all field evaluations of transport properties, pre-conditioning of the specimens is critical. Dhir et al. [58] recommend using the ISAT apparatus to first pull a vacuum on the surface to be tested prior to measuring the absorption of the water. Nolan [59] has evaluated four different preconditioning methods for use onsite: 1) vacuum, 2) hot air, 3) pressurized dried compressed air, and 4) solvent replacement using diethyl ether. In general, very little water was removed by any of the methods, as measured RH values were still in the range of 95 % to 99 %. In summary, while suitable field techniques have been developed, the interpretation of results is often difficult and sometimes impossible due to the highly variable moisture content of field concrete. For example, a saturated field concrete of poor quality may exhibit a similar measured sorptivity as an unsaturated high-quality concrete.

[1] Certain commercial equipment is identified by name in this report. In no case does such identification imply endorsement by the National Institute of Standards and Technology, nor does it imply that the products are necessarily the best available for the purpose.

5.2 Permeability

Onsite testing of concrete permeability can be conveniently classified into two types of tests: those which measure permeability as flow emanating from a hole drilled in the concrete, and those which measure permeability as flow emanating from the surface of the concrete. Initial development work in the former case was performed by Figg [60, 61]. He suggested drilling a 5.5 mm diameter hole to a depth of about 30 mm, applying a seal (stopper), and then using a hypodermic needle connected to a manometer to apply either a negative (air) or positive (water) pressure to the system. Flowrates or pressure decay are monitored and a permeability "coefficient" is determined as the time required for a fixed pressure increase or fixed amount of flow. These times can be converted to intrinsic permeabilities using equations originally developed in geotechnical work and presented by Figg in reference [61].

The initial 5.5 mm diameter hole was subsequently found to be far too small to provide a representative volume of concrete for testing, resulting in very high coefficients of variation. Cather et al. [62] suggested an increase in the hole diameter to 10 mm and other researchers have used even larger holes (20 mm for example [63]). In a variant of this test method, Paulmann [4] suggests measuring the air flow from the concrete surrounding the drilled hole to assess if and when steady state conditions are actually achieved. For water permeability, Meletiou et al. [25] have modified the basic Figg test to achieve water flow from only a portion of the hole's depth and developed an appropriate equation (Equation 13) for evaluating intrinsic permeability from the cumulative water flow vs. time behavior.

For the surface permeability tests, a chamber is sealed to the concrete surface and air or water flow monitored, in a setup similar to that used for the ISAT test shown in Fig. 5. Lydon and Odaallah [64] suggest monitoring the pressure decay time using a fixed volume of nitrogen gas at a pressure of 1 MPa. The pressure decay vs. time curve provides a measure of the permeability of the concrete. Torrent [65] has developed a commercially-available apparatus in which a vacuum is applied to the chamber attached to the concrete surface and the time required for the pressure to return to atmospheric is evaluated. His system employs a two-chamber vacuum cell in an attempt to create one-dimensional flow conditions. The AutoClam, described previously for sorption measurements, can also be used to evaluate either air or water permeability of the surface concrete [57]. This device provides a permeability index (either the pressure decay rate or volumetric flow rate), as opposed to a value for the intrinsic permeability of the concrete. The laboratory test developed by Schonlin [46] and presented previously in this report can also be used in the field. The sample is first dried using hot air, the vacuum chamber is attached to the surface, and the pressure decay monitored to provide a permeability index [4].

Under a contract from the Strategic Highway Research Program (SHRP), Whiting and Cady [66] developed a surface air flow (SAF) device for evaluating air permeability onsite. The equipment is attached directly to the concrete surface and the rate of air flow under vacuum conditions is assessed. Under the recommended operational procedures, the quality of the concrete to a depth of about 12 mm can be assessed using this technique. Results are reported as the air flowrate in ml/min. The test requires a dry concrete, sometimes difficult to achieve under field conditions. In the SHRP study, the use of a hot air gun and an infrared heater to dry the concrete were both evaluated with limited success [66]. This testing equipment has been used by several state DOT's and some of their evaluations are available at the SHRP Product Evaluation Web site [67]. In addition, the test method has been standardized by AASHTO under designation TP26-94, "Standard Test Method for

Determining the Relative Permeability of Concrete by Surface Air Flow" [68].

5.3 RH and Moisture Content Assessment

Because suitable in-situ preconditioning of field concrete is still lacking, an alternative is to measure the transport properties of the concrete in its "as is" condition and attempt to quantify this "as is" condition. Two parameters of interest are the internal relative humidity of the concrete and its moisture content.

The internal relative humidity changes with the ambient relative humidity and drying and wetting of the concrete. In addition, particularly in high performance concretes, the internal relative humidity is reduced due to chemical shrinkage and self-desiccation occurring during hydration [69]. To assess internal relative humidity, typically, a hole is drilled in the concrete and a relative humidity probe is sealed into the hole [35, 48, 70]. Even under ideal conditions, the response time of these probes can be "inconveniently slow (on the order of hours)" at relative humidities above 80 % [71]. Care must also be taken when using these probes to frequently perform a calibration as their response tends to drift over time, typically over saturated salt solutions [35, 71]. Parrott measured relative humidities between 50 % and 100 % for concretes exposed outdoors, the lower values being found for concretes sheltered from the rain. Conversely, for specimens exposed to natural weathering in Madrid, Andrade et al. [72] measured relative humidity values generally between 40 % and 80 %, with occasional values over 90 % during periods of rain.

As mentioned earlier, unfortunately, there is not a one-to-one relationship between internal relative humidity and moisture content of concrete due to the significant hysteresis in the adsorption/desorption isotherms. Depending on the concrete, the moisture content could vary by a factor of two or more at the same relative humidity during drying and wetting conditions [29]. To directly evaluate moisture content, basically two techniques have been proposed. Parrott [71] proposes placing small cement paste prisms at various depths in the concrete and periodically assessing their change in mass. If the cement paste is of a similar w/c ratio and degree of hydration as that in the concrete, its moisture history should closely predict that of the surrounding concrete. While this seems to be a straightforward assumption, the complexity of the concrete microstructure is such that neither the interfacial transition zone cement paste nor the bulk cement paste has the nominal w/c ratio of the concrete [73].

The second approach is to infer moisture content from a non-destructive in-situ measurement, typically an electrical measurement. Early developments in using electrical measurements to assess the moisture content of concrete in the U.S. date from the 1930s [74]. Electrical resistance measurements between sets of embedded probes were used to quantify the moisture state of a variety of laboratory and field concretes. For the field concretes, using the probes, it was observed that concrete gains moisture during wetting at a much faster rate than it loses it during subsequent drying. The technique was rediscovered in the late 1960s [75] and early 1970s [76] and used to monitor the progress of the wetting front in a concrete exposed to water. Woelfl and Lauer [77] found that for a given set of concrete mixture proportions, electrical resistivity decreased with increasing moisture content. To try to avoid polarization effects, these authors employed an alternating current at frequencies above 50 Hz. More recently, the technique has been examined extensively by McCarter and his colleagues [78, 79, 80]. In one case [79], the resistance readings of an embedded probe

measured at a frequency of 5 kHz were used to monitor the depth of water penetration with time during an ISAT evaluation of sorptivity. These results indicated that the water penetration front becomes more diffuse with depth and that a combination of mass gain and electrical measurements could provide a non-destructive measure of the porosity of the concrete as a function of depth in real time. One problem for field use is that the concrete conductivity/resistivity is strongly dependent on the resistivity of its pore solution, which will depend on cement composition, mixture proportions, and exposure environment, as well as the saturation state of the concrete. Thus, absolute comparison between widely differing kinds of concrete is difficult.

6 Relationships Between Transport and Durability

Kropp has provided two excellent summaries of the relations between transport properties and durability of concrete [4, 81]. Much of the research in this area has focused on carbonation (perhaps because it is mechanistically better understood than other degradation processes), with only a few studies on other deterioration modes such as sulfate attack or alkali-silica reaction.

6.1 Carbonation

Parrott [82] has concluded that under normal environmental conditions, carbonation is controlled by gas diffusion through the empty pores in the exposed surface layer of the concrete. Since both gas permeabillity and sorptivity measure the resistance of these pores to transport processes, it not too surprising that numerous researchers have correlated carbonation depths with air permeabilities and sorptivities [2, 7, 8, 9, 83, 84, 85]. Ballim [9] correlated 10 month carbonation depths with 28 day oxygen permeabilities and water sorptivities and found that both measures provided correlation coefficients on the order of 0.95 for a specific concrete. However, the specific relationship is dependent on the binder type (ordinary portland cement, cement with fly ash, cement with ground, granulated blast-furnace slag), so that no single value can be specified as a durability index. To circumvent this problem, Ballim suggests combining a general single-value durability index with a minimum strength requirement. The minimum strength requirement will ensure that an adequately low w/c ratio is used in the concrete to achieve appropriate performance in properly cured blended cement concretes.

Dhir et al. [7] examined the relationship between air permeability and carbonation depth after 20 weeks of accelerated carbonation in a 4 % CO_2, 50 % RH environment. Assuming that 1 week of exposure under the accelerated conditions corresponds to 15 months of normal exposure, they derived the following equation relating carbonation depth to intrinsic permeability:

$$D_t = (\frac{t_y}{20})^{\gamma}(22.8 \times log(10^{17} \times k_l) - 6.9) \tag{17}$$

where D_t is the carbonation depth in mm after time t_y in years, k_l is the intrinsic permeability (measured on specimens dried at 105 °C), and γ is a constant taking a value of 0.4 for concretes with w/c>0.6, and 0.5 otherwise. An additional relationship between the Figg permeability index [60] and carbonation depth is also derived by Dhir et al. [7].

Parrott [86] has derived the following relationship between carbonation depth and oxygen permeability (samples preconditioned at 60 % RH):

$$D_t = \frac{64 \times (10^{16} \times k_l)^{0.4} t_y^n}{a_c^{0.5}} \tag{18}$$

where a_c is the calcium oxide content of the cement (in kg/m^3 of cement matrix) and n is an attenuation factor, varying from about 0.2 for damp concrete to 0.5 for dry concrete. This form of the equation is consistent with that derived analytically by Hilsdorf and presented by Kropp [4] where penetration depth varies with the square root of time and permeability to some power.

Balayssac et al. [84, 85] have observed a linear relationship between initial sorptivity (total quantity of water absorbed in the first hour of an absorption test normalized by the exposed surface area) and carbonation depths after 180 days and 360 days exposure. Parrott [83] observed a similar relation between depth of carbonation and water absorbed after 4 h of absorption testing for concretes exposed indoors and outdoors for 1.5 years. Conversely, Ballim and Lampacher [87] found little or no correlation between air permeability or sorptivity and carbonation for exposed bridge concrete specimens between 19 years and 30 years of age. Perhaps, at these later ages, the carbonation process has modified the pore structure substantially, so that the transport properties measured on the degraded concrete are unrepresentative of those present when the degradation was in its early stages.

In addition to transport properties, carbonation rates will be influenced by the composition of the cements (hence the a_c term in Equation 18) and the densification of the pore system that occurs as calcium carbonate replaces calcium hydroxide at the reaction front. This latter effect is due to the fact that the molar volume of calcium carbonate is greater than that of calcium hydroxide.

6.2 Sulfate Attack

Sulfates transported into the concrete from the environment can result in cracking and scaling of the concrete surface. In a saturated state, the major transport mechanism will be diffusion; in an unsaturated concrete, transport by capillary sorption will also be significant. Kropp [4] presents data of Goncalves showing that the weight change during exposure to a sulfate solution correlates with conventional capillary absorption measurements. In addition, those specimens that absorbed more of the solution exhibited more deterioration, evaluated visually.

A detailed model for sulfate attack has been developed by Atkinson and Hearne [88]. In their equation, the degradation rate is proportional to the diffusivity of sulfate ions in the concrete. Since permeability is generally proportional to diffusivity to some power [4, 26], the degradation rate should be proportional to gas permeability, for example, to some power. For our purposes, the key feature of the Atkinson and Hearne model is the prediction of the depth at which spalling will occur. Based on an equivalence between the strain energy developed in the concrete due to the expansive reactions and its fracture energy, they present the following equation for the spalling depth [88]:

$$X_{spall} = \frac{2\alpha\gamma_f(1-\nu)}{E(\beta C_E)^2} \tag{19}$$

where X_{spall} is the thickness of the spalled layer, α is a roughness factor for the fracture path (assigned a value of 1 in [88]), γ_f is the fracture surface energy of the concrete, ν is Poisson's ratio, E is Young's modulus of the concrete, β is the linear strain caused by one mole of sulfate reacting (1.8×10^{-6} m^3/mole), and C_E is the concentration of reacted sulfate as ettringite. This latter term will be controlled by the rate of sulfate ingress (due either to diffusion or sorption) and the availability of the aluminate phases within the concrete.

Equation 19 can be used in combination with Equation 2 or Equation 4 to estimate the service life for a concrete exposed to sulfate attack in the following manner. Let us assume that the primary mechanism for sulfate ingress is sorption (as opposed to diffusion in the original development of Atkinson and Hearne) and further assume that the sulfate concentration in the sorbing fluid is equivalent to that in the external environment. This is a simplification, because McCarter et al. [89] have shown that, for the case of chloride ions, the chloride ingress front lags behind the absorption front, due to interactions of the chloride ions with the cement matrix. We will require an estimate of the "time-of-wetness" (TOW- the time during which the surface of the concrete is wet) distribution of the concrete. One way to obtain the TOW would be to use the distribution of the durations of rainfall during the year. For each rain period of duration t_i, Equation 2 or 4 can be used to calculate the depth of penetration, d_i, of the sulfate-containing water during the rain exposure. Then, for any depth, x, we have:

$$C_E(x,t) = F \sum C^i_{ext} \times f \times H_f(d_i - x) \tag{20}$$

where F is a conversion between external sulfate concentration and ettringite formation, C_{ext} is the sulfate concentration of the external solution in mol/m^3, and H_f is the Heaviside function, taking values of 1 when $(d_i - x) > 0$ and 0 otherwise. For the value of $C_E(x)$ at each depth x, Equation 19 can be used to compute a corresponding value of X_{spall}. If $X_{spall} < x$, spalling will occur. If this cumulative spalling depth is greater than the value established for the end of service life, the calculation is complete and the final value of t is the estimated service life. If not, multiple spallings are required to end the service life, and the calculation is continued with the current spalling depth taken as the new $x = 0$ surface for subsequent sorption calculations using Equation 20. An example of this calculation is provided in Appendix A. This is a conservative estimate in that we are applying the worst case scenario that the surface pores have adequate time to empty out before the next rain/sorption cycle, thus maximizing the ingress of sulfate.

6.3 Alkali-Silica Reaction

For alkali-silica reactions (ASR), the deleterious expansion that occurs is due to the formation of a gel product from the reaction of alkalis present in the cement and/or originating from the exposure environment with (reactive) siliceous aggregates (or perhaps with agglomerated silica fume particles [90]). Thus, the compositions of the cement and aggregate components of the concrete mixture proportions are both important. However, in all cases, the presence of moisture is critical to the formation of a "swelling" gel [91], which leads to stress generation and cracking. Recently, Capra and Bournazel [92] have presented a model for the expansion due to ASR of the form:

$$\epsilon^{asr} = \left(\frac{RH}{100}\right)^m \times \frac{\epsilon_0}{A_0} \times \left(1 - A_0 - e^{tK_{0e}^{\frac{-E_a}{RT}}}\right) \times f(\sigma_{conc}) \tag{21}$$

where ϵ^{asr} is the expansion due to ASR, m typically is given a value of 8, ϵ_0 and A_0 represent fitting constants for the relationship between expansion and fraction of the alkalies reacted, K_0 is the reaction rate constant for alkali consumption, and $f(\sigma_{conc})$ represents a function of the stress state of the concrete. Here, it is assumed that the reaction kinetics are first order with respect to the alkalies and do not depend on the reactive aggregate content (i.e., sufficient reactive aggregates are present to consume all of the alkalies).

Since an expansive reaction is once again regulating the degradation, one can also envision a formulation similar to that developed above for the case of sulfate attack. For sulfate attack, the expansive reaction of the paste results in spalling, while for ASR, the expansive reaction at the aggregate surfaces results in internal cracking (and possible spalling). To model ASR degradation in this manner, it will be necessary to estimate the linear strain caused by the formation of 1 mol of alkali-silica reaction products, and the conversion factor from alkali ion concentration to moles of reaction product. These parameters could vary greatly from one concrete to another depending in the former case on the spatial distribution and surface area of the reactive aggregates and in the latter case on the specific chemical composition of the ASR gel.

In this case, the equivalent C_E term for Equation 19 will be composed of two components, one for the initial alkali content of the cement and the other for the alkalis which penetrate into the concrete from the external exposure environment. Since the components needed for alkali-silica reaction (alkalis, reactive aggregates, and water) may be present from time zero, account must also be made for the expansion that will occur during the initial hydration of the cement, where there is a competition for the available mixing water between the hydration and the alkali-silica reactions. As this research project develops, a more detailed model relating alkali-silica degradation to sorptivity will be developed.

6.4 Freeze/Thaw Damage

For significant freeze/thaw damage to occur in non-air entrained concrete, the concrete must be saturated above 90 % [69]. Thus, the penetration of water into the concrete via sorption and diffusion may have major effects on its freeze/thaw performance. Basheer et al. [8] have observed good correlation between concrete performance in ASTM C666, Procedure B freeze/thaw testing [93] and sorptivities and air permeabilities determined using the AutoClam testing apparatus. Kropp [4] also provides some data from other studies showing correlation between mass loss during freeze/thaw testing and air permeabilities and water absorption.

Recently, Bager and Jacobsen [94] have proposed a conceptual model for the scaling damage of non-air entrained concrete exposed to freeze/thaw cycles. During the first few cycles of testing (or field exposure), the paste expands due to ice formation, creating a circumferential crack around each aggregate. Initially, these cracks are air-filled, but over time, due mainly to the sorptivity of the concrete, they become water-filled. When the cracks become saturated and the water within them freezes, they produce a radial crack pattern throughout the cement paste and substantial scaling results. The presented model is quite consistent with the experimental data (dilation, ultrasonic pulse velocity, scaling, and water uptake) for three different w/c ratio concretes presented in [94]. Thus, sorptivity is seen to play a major role in the freeze/thaw scaling of field concrete. The situation is further complicated by the fact that the sorptivity of a concrete undergoing freeze/thaw cycling may

be different from that of a concrete tested at room temperature conditions in the laboratory [95]. Of course, the pore and crack network structure is changing during the freeze/thaw cycling, and a variety of other mechanisms (hydraulic pressure from external ice, suction due to melting ice, and vapor diffusion from gel to capillary pores [95]) are active during the actual freeze/thaw exposure. Thus, an additional sorptivity test under freeze/thaw conditions may need to be developed to better evaluate the freeze/thaw resistance of a specific concrete.

If one's main interest is scaling resistance, a formulation similar to that developed for sulfate attack by Atkinson and Hearne [88] and outlined above could be employed. The major difference is that the deleterious expansion in this case is due to the volumetric expansion that occurs during the freezing of water instead of the formation of expansive reaction products. In the simplest form, one would be interested in the time required for the cracks surrounding each aggregate at the critical scaling (spalling) depth to saturate. An estimate of the volume occupied by these cracks for any aggregate gradation of interest can be easily obtained using the NIST concrete microstructure model [96].

For this case, the βC_E term in Equation 19 should be replaced by the expansion caused by ice formation. Since there is a 9.1 % volume expansion during freezing [81], this term could become a linear expansion of about 3 %. This value should be multiplied by the porosity fraction of the concrete (including the cracks) at saturation. In this case, the worst case scenario is that the surface concrete remains saturated after initial penetration, so that all sorption is cumulative. Then, the cumulative penetration depth is simply given by:

$$d_{cum} = B\sqrt{\sum_i t_i} \tag{22}$$

where B is adjusted for the additional porosity due to the circumferential cracks around each aggregate. This cumulative depth of penetration can be compared to the spalling depth calculated via the modified form of Equation 19 and the service life estimated as the first time (freezing cycle) when $X_{spall} < d_{cum}$. This is also a worst case scenario because it assumes that there are no air voids or other defects to reduce the expansion and that all of the ice expansion is directly translated into strain of the concrete.

6.5 Acid Attack and Leaching

Because of the highly basic nature of the pore solution of concrete, acids and even neutral groundwater can substantially modify the pH of the pore solution, leading to the progressive dissolution of calcium hydroxide and calcium silicate hydrates (*C-S-H*) from the cement paste matrix. Once dissolved, these species will generally diffuse from the interior of the concrete toward the exposed surface. Thus, while sorption may result in the ingress of a deleterious fluid, the leaching rate will most likely be determined by the diffusivity of the concrete, and thus by the permeability of the concrete raised to some power. Most degradation models predict that the deteriorated layer thickness will vary with either time or the square root of time [4], depending on whether or not a protective product layer is formed by the acid dissolution reactions. In either case, concretes of low sorptivity and permeability should perform better in terms of preventing both ingress of the deleterious external solution and removal by diffusion of the leached species.

7 Recommended Approach

Because of the difficulties of interpreting field measurements due to the highly variable moisture conditions of the concrete, for this study, it is proposed to conduct laboratory evaluations of pre-conditioned field specimens. Furthermore, because of the long times needed to pre-condition and evaluate water permeabilities, the initial testing program will be limited to evaluations of gas permeability and water sorptivity. Initially, one of the pre-conditioning regimes of Parrott [14] (4 days of 50 °C oven drying followed by 3 days of sealed drying also at 50 °C) will be evaluated. This will hopefully produce concrete specimens with internal relative humidities near 60 %, a value typical of field exposure. An additional benefit of laboratory testing relative to in-situ field testing is that it is much easier to maintain one-dimensional flow boundary conditions using the tests shown in Figs. 3 and 4.

The following is a general outline for the proposed testing program, illustrated in the flowchart in Fig. 6:

1. obtain 75 mm diameter by 150 mm (or 100 mm diameter by 200 mm) cores from the field concrete to be evaluated
2. optionally, assess the carbonation depth of each specimen using the phenolphthalein indicator test
3. slice the cores across the longitudinal axis into equal quarters
4. evaluate the initial mass of each specimen and the mass after sealing the lateral edges of the specimens to ensure uni-directional drying
5. vacuum saturate the specimens in limewater and evaluate the saturated mass of each
6. pre-condition the samples following the regime of Parrott or a variant thereof
7. evaluate the dried mass and internal relative humidity of each specimen
8. measure the gas permeability using equipment similar to that shown in Fig. 4
9. measure sorptivity of the "top" surface of each specimen using the experimental setup shown in Fig. 3
10. optionally, measure the sorptivity of the "bottom" surface of each specimen
11. optionally, vacuum saturate the specimen and evaluate its mass
12. optionally, measure the rapid chloride permeability of each specimen
13. dry each specimen to a constant mass in an oven at 105 °C
14. evaluate the 105 °C-dried mass of each specimen
15. evaluate the gas permeability of the 105 °C-dried specimen

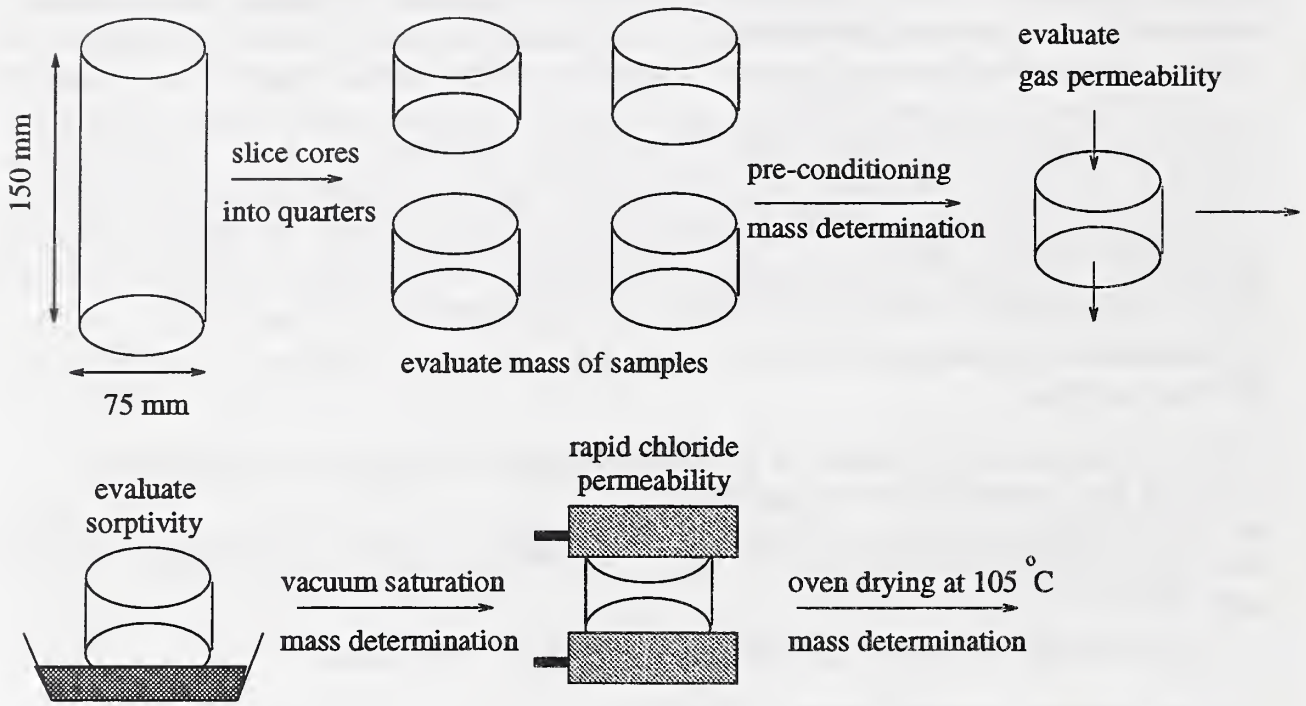

Figure 6: Flowchart illustrating proposed experimental protocol.

16. apply developed service life models based on measured transfer coefficients, intended exposure environment, and anticipated degradation modes.

All laboratory measurements will be conducted at (23 $\pm$ 2) °C. It is estimated that this testing regime will require between 10 days and 20 days to evaluate a series of specimens. During all laboratory procedures, all possible precautions to avoid further carbonation of the specimens will be taken. Nitrogen will be used as the flowing gas for the gas permeability evaluations.

There are a number of questions which must be addressed as the testing procedure is developed, including:

1. What fluid should be used in the sorption tests (distilled water, calcium hydroxide-saturated water, or an organic fluid such as ethylene glycol or 1-propanol)?

2. Is re-pre-conditioning of the specimens needed following the gas permeability test?

3. What is the minimum time needed to accurately determine a sorptivity or penetration coefficient (4 h, 8 h, or 24 h)?

4. Does not taping one of the faces of the disc specimen prior to sorptivity evaluation significantly affect the results? What if we place a polystyrene cap over this surface instead? This modification would allow us to rapidly evaluate the sorptivities of both the top and bottom surfaces of a specimen to look for differences.

5. Is the proposed pre-conditioning regime sufficient to produce a specimen with a homogeneous moisture distribution?

6. Are the samples thick enough (37.5 mm) to avoid significant finite size effects? Is this thickness greater than 3 times the generally used maximum aggregate diameter? Can we use even thinner specimens which will equilibrate faster in the pre-conditioning environment?

7. Can we avoid further carbonation during the specimen handling, preparation, and testing? We can examine this by measuring the carbonation depths before and after the testing program.

Initial efforts will concentrate on a comprehensive evaluation of the pre-conditioning regime of Parrott [14]. A wide variety of concrete cores will be exposed to a controlled temperature and humidity environment (50 °C and 80 % RH) for three to four days, and then stored in sealed bags at the same temperature to allow for moisture equilibrium to be approached. After pre-conditioning, the mass of each specimen will be determined and its internal relative humidity measured. If possible, the water distribution will be directly quantified by measuring the hydrogen content as a function of depth, using nuclear techniques available at the NIST Cold Neutron Research Facility, or by using X-ray equipment available at the Technical University of Denmark, a partner in the NIST Partnership for High Performance Concrete Technology program.

8 Conclusions

A review of the state-of-the-art with respect to transport properties and durability of concrete has been presented. While adequate field tests have been developed, all are greatly influenced by the moisture condition of the concrete being tested. Since an accurate quantitative assessment of the moisture condition of field concrete is not yet possible, it is recommended that for this study, cores be taken and conditioned in the laboratory prior to assessment of gas permeability and water sorptivity. Laboratory testing also allows for the convenient maintenance of one-dimensional flow boundary conditions, greatly simplifying the analysis. A preliminary testing program and testing guidelines have been recommended and a set of testing issues requiring resolution identified. Equations for preliminary durability predictions based on these transfer coefficients and a knowledge of the exposure environment have been presented. The particular importance of sorptivity in providing water and/or deleterious ions needed for degradation in partially saturated concrete has been highlighted.

9 Notation

A exposed surface area (m^2)

A_0 minimum fractional alkali comsumption necessary to cause expansion

a_c calcium oxide content of cement (kg/m^3 cement matrix)

b constant for Klinkenberg correction for gas permeability

B penetration coefficient ($m/s^{0.5}$)

C constant

C_E concentration of reacted sulfate as ettringite (mol/m^3)

C_{ext} sulfate concentration in external solution (mol/m^3)

d penetration depth (m)

D_t carbonation depth (mm)

E Young's modulus (GPa or N/m^2)

E_a activation energy (kJ/mol)

f porosity fraction (m^3 porosity/m^3 concrete)

F conversion between external ion (sulfate) concentration and expansive reaction product (ettringite) formation (mol/mol)

g gravitational constant (m^2/s)

h height in capillary tube (m)

H length of test section in drilled hole (m)

H_f Heaviside function $H_f(x)$=1 when $x > 0$ and 0 otherwise

k (k_g and k_l) permeability coefficient (m^2)

K transport coefficient (m^2/s)

K_0 rate constant for alkali comsumption

L diameter of wetting source for sorption test (m)

M mass (kg)

m exponent relating ASR expansion to relative humidity

n constant- attenuation factor

P pressure (N/m^2)

Q volumetric flow rate (m^3/s)

r_h test hole radius (m)

r_p pore radius (m)

R universal gas constant (8.314 kJ/(mol-K))

RH relative humidity

s capillary tube cross section (m^2)

S sorptivity coefficient ($m/s^{0.5}$)

t time (s)

t_i time duration of a period of rain (s)

t_y time (years)

T absolute temperature (K)

x specimen thickness or depth (m)

X_{spall} spalled thickness (m)

V volume of air or fluid (m^3)

V_m molar volume (m^3/mol)

W total intake of water per unit mass (kg/kg)

α roughness factor for fracture path

β linear strain caused by one mole of sulfate reacted (m^3/mol)

ϵ^{asr} expansion due to ASR reatcion (%)

ϵ_0 fictitious negative expansion at time zero (%)

η dynamic viscosity (N-s/m^2)

γ constant

γ_f fracture surface energy of concrete (J/m^2 or N/m)

ν Poisson's ratio (e.g., 0.3)

π 3.1415926

ρ density (kg/m^3)

σ surface tension (N/m)

σ_{conc} stress state of the concrete

θ moisture content

ω molecular mass of air (kg/mol)

ξ saturation

10 Useful Constants

Dynamic viscosity of water at 20 °C = $1.0*10^{-3}$ N-s/m^2[20]

Dynamic viscosity of nitrogen at 20 °C = $1.78*10^{-5}$ N-s/m^2[97]

Dynamic viscosity of oxygen at 20 °C = $2.02*10^{-5}$ N-s/m^2[44]

Surface tension of water at 20 °C = 0.07275 N/m[97]

11 Acknowledgements

This study is being funded by the Federal Highway Administration. The assistance of the contract office technical representatives, Dr. Stephen Forster and Marcia Simon, is greatly appreciated. The assistance of Kenneth Snyder and Xiuping Feng (BFRL/NIST) in setting up and evaluating the gas permeability equipment is appreciated.

During the initial stages of this project, Dr. James Clifton passed away suddenly. The other authors of this report deeply appreciate the encouragement, sound technical expertise, and strategic planning which he has shared with them over the years at NIST. Jim was instrumental in defining the scope of this project with the FHWA and we hope our efforts will do justice to his insightful planning.

12 References

[1] Kreijger, P.C., "The Skin of Concrete: Composition and Properties," Materials and Structures, **17** (100), 275-283, 1984.

[2] Bentur, A., and Jaegermann, C., "Effect of Curing and Composition on the Properties of the Outer Skin of Concrete," Journal of Materials in Civil Engineering, **3** (4), 252-262, 1990.

[3] Dhir, R.K., Hewlett, P.C., and Chan, Y.N., "Near Surface Characteristics of Concrete: Intrinsic Permeability," Magazine of Concrete Research, **41** (147), 87-97, 1989.

[4] Performance Criteria for Concrete Durability, Ed. J. Kropp and H.K. Hilsdorf (E & FN Spon, London, 1995).

[5] Dias, W.P.S., "Durability Indicators of OPC Concretes Subject to Wick Action," Magazine of Concrete Research, **45** (165), 263-274, 1993.

[6] Ho, D.W.S., Potter, R.J., Beresford, P.D., and Lewis, R.K., "Durability of Concrete- A Research Project," CIA Biennial Conference, pp. 1-6, Melbourne, Australia, 1985.

[7] Dhir, R.K., Hewlett, P.C., and Chan, Y.N., "Near Surface Characteristics of Concrete: Prediction of Carbonation Resistance," Magazine of Concrete Research, **41** (148), 137-143, 1989.

[8] Basheer, P.A.M., Montgomery, F.R., and Long, A.E., "Factorial Experimental Design for Concrete Durability Research," Proc. Instn. Civ. Engrs. Structs. & Bldgs., **104**, 449-462, 1994.

[9] Ballim, Y., "Towards an Early-Age Index for the Durability of Concrete," in CONCRETE 2000: Economic and Durable Construction through Excellence, Ed. R.K. Dhir and M.R. Jones (E & FN Spon, London, 1994) pp. 1003-1012.

[10] Alexander, M.G., and Ballim, Y., "Experience with Durability Testing of Concrete: A Suggested Framework Incorporating Index Parameters and Results from Accelerated Durability Tests," in Proceedings of the Third Canadian Symposium on Cement and Concrete, 248-263, 1993.

[11] Hall, C., "Barrier Performance of Concrete: A Review of Fluid Transport Theory," Materials and Structures, **27**, 291-306, 1994.

[12] Martys, N.S., "Survey of Concrete Transport Properties and Their Measurement," NISTIR **5592**, U.S. Department of Commerce, 1995.

[13] Garboczi, E.J., "Permeability, Diffusivity, and Microstructural Parameters: A Critical Review", Cement and Concrete Research, **20**, 591-601, 1990.

[14] Parrott, L.J., "Moisture Conditioning and Transport Properties of Concrete Test Specimens," Materials and Structures, **27**, 460-468, 1994.

[15] Ho, D.W.S., and Lewis, R.K., "The Water Sorptivity of Concretes: The Influence of Constituents under Continuous Curing," Durability of Building Materials, **4**, 241-252, 1987.

[16] Sosoro, M., "Transport of Organic Fluids Through Concrete," Materials and Structures, **31**, 162-169, 1998.

[17] Hall, C., and Yau, M.H.R., "Water Movement in Porous Building Materials- IX. The Water Absorption and Sorptivity of Concretes," Building Environment, **22**, 77-82, 1987.

[18] Martys, N.S., and Ferraris, C.F., "Capillary Transport in Mortars and Concrete," Cement and Concrete Research, **27** (5), 747-760, 1997.

[19] Wilson, M.A., Taylor, S.C., and Hoff, W.D., "The Initial Surface Absorption Test (ISAT): An Analytical Approach," Magazine of Concrete Research, **50** (2), 179-185, 1998.

[20] Bamforth, P.B., "The Relationship Between Permeability Coefficients for Concrete Obtained Using Liquid and Gas," Magazine of Concrete Research, **39** (138), 3-11, 1987.

[21] Klinkenberg, L.J., "The Permeability of Porous Media to Liquids and Gases," Drilling and Production Practice (American Petroleum Institute, New York, 1941) pp. 200-214.

[22] Abbas, A., Carcasses, M., and Ollivier, J.-P., "Gas Permeability of Concrete in Relation to its Degree of Saturation," Materials and Structures, **32**, 3-8, 1999.

[23] Yssorche, M.P., Bigas, J.P., and Ollivier, J.P., "Mesure de la Permeabilite a l'air des Betons au Moyen d'un Permeametre a Charge Variable," Materials and Structures, **28**, 401-405, 1995.

[24] Ballim, Y., "A Low Cost, Falling Head Permeameter for Measuring Concrete Gas Permeability," Concrete Beton, 13-18, November 1991.

[25] Meletiou, C.A., Tia, M., and Bloomquist, D., "Development of a Field Permeability Test Apparatus and Method for Concrete," ACI Materials Journal, **89** (1), 83-89, 1992.

[26] E.J. Garboczi, "Permeability, Diffusivity, and Microstructural Parameters: A Critical Review," Cement and Concrete Research, **20**, 591-601, 1990.

[27] Bentz, D.P., Quenard, D.A., Baroghel-Bouny, V., Garboczi, E.J., and Jennings, H.M., "Modelling Drying Shrinkage of Cement Paste and Mortar: Part I. Structural Models from Nanometres to Millimetres," Materials and Structures, **28**, 450-458, 1995.

[28] Winslow, D.N., and Lui, D., "The Pore Structure of Paste in Concrete," Cement and Concrete Research, **20**, 227-235, 1990.

[29] Baroghel-Bouny, V., "Caracterisation Microstructurale et Hydrique des Pates de Ciment et des Betons Ordinaires et a Tres Hautes Performances," Ph. D. Thesis, L'ecole Nationale des Ponts et Chaussees, Paris, France, 1994.

[30] Baroghel-Bouny, V., "Texture and Moisture Properties of Ordinary and High-Performance Concrete Materials," in Concrete: From Material to Structure, Ed. J.P. Bournazel and Y. Malier, RILEM, 144-165, 1998.

[31] Tsimbrovska, M., "Degradation des Betons a Hautes Performances Soumis a des Temperatures Elevees: Evolution de la Permeabilite en Liaison avec la Microstructure," Ph. D. Thesis, L'universite Joseph Fourier, Grenoble, France, 1998.

[32] Delagrave, A., Marchand, J., and Pigeon, M., "Influence of Microstructure on the Tritiated Water Diffusivity of Mortars," Advanced Cement-Based Materials, **7**, 60-65, 1998.

[33] Bentz, D.P., Garboczi, E.J., and Lagergren, E.S., "Multi-Scale Microstructural Modelling of Concrete Diffusivity: Identification of Significant Variables," Cement, Concrete, and Aggregates, **20** (1), 129-139, 1998.

[34] Buenfeld, N.R., and Okundi, E., "Effect of Cement Content on Transport in Concrete," Magazine of Concrete Research, **50** (4), 339-351, 1998.

[35] Hedenblad, G., "Moisture Permeability of Mature Concrete, Cement Mortar, and Cement Paste," Ph. D. Thesis, Lund Institute of Technology, Lund, Sweden, 1993.

[36] Ferraris, C.F., unpublished results.

[37] Ballim, Y., "Low-Cost Laboratory Test Methods for Demonstrating the Relationship Between Concrete Practice and Durability to Undergraduate Students," in Concrete Technology in Developing Countries, Ed. A. Yeginobah, 271-278, 1996.

[38] Ballim, Y., "Curing and the Durability of OPC, Fly Ash and Blast-Furnace Slag Concretes," Materials and Structures, **26**, 238-244, 1993.

[39] Kelham, S., "A Water Absorption Test for Concrete," Magazine of Concrete Research, **40** (143), 106-110, 1988.

[40] Sabir, B.B., Wild, S., and O'Farrell, M., "A Water Sorptivity Test for Mortar and Concrete," Materials and Structures, **31**, 568-574, 1998.

[41] DeSouza, S.J., Hooton, R.D., and Bickley, J.A., "Evaluation of Laboratory Drying Procedures Relevant to Field Conditions for Concrete Sorptivity Measurements," Cement, Concrete, and Aggregates, **19** (2), 59-63, 1997.

[42] McCarter, W.J., "Influence of Surface Finish on Sorptivity of Concrete," Journal of Materials in Civil Engineering, **5** (1), 130-136, 1993.

[43] Hearn, N., and Mills, R.H., "A Simple Permeameter for Water or Gas Flow," Cement and Concrete Research, **21**, 257-261, 1991.

[44] Kollek, J.J., "The Determination of the Permeability to Oxygen by the Cembureau Method- A Recommendation," Materials and Structures, **22**, 225-230, 1989.

[45] Martin, G.R., "A Method for Determining the Relative Permeability of Concrete Using Gas," Magazine of Concrete Research, **38** (135), 90-94, 1986.

[46] Schonlin, K., and Hilsdorf, H.K., "Permeability as a Measure of Potential Durability of Concrete- Development of a Suitable Test Apparatus," ACI SP 108-6, Permeability of Concrete, Ed. D. Whiting and A. Walitt (ACI, Detroit, 1988) pp. 99-115.

[47] Scherer, G.W., private communication, Jan. 1999.

[48] Parrott, L.J., "Factors Influencing Relative Humidity in Concrete," Magazine of Concrete Research, **43** (154), 45-52, 1991.

[49] Quenard, D.A., and Carcasses, M., "Les Resultats Des Essais Croises AFREM Permeabilite," Journee Techniques AFPC-AFREM, Durabilite des Betons, 41-58, 1997.

[50] Galle, C., Daian, J.F., and Pin, M., "Trasnfert des Gaz dans les Materiaux Cimentaires: Experimentation et Modelisation du Couplage Microstructure/ Saturation en Eau/ Permeabilite," Journee Techniques AFPC-AFREM, Durabilite des Betons, 207-219, 1997.

[51] Levitt, M., "The ISAT - A Non-Destructive Test for the Durability of Concrete," British Journal of N.D.T., **13** (4), 106-112, 1971.

[52] Price, W.F., and Bamforth, P.B., "Initial Surface Absorption of Concrete: Examination of Modified Test Apparatus for Obtaining Uniaxial Absorption," Magazine of Concrete Research, **45** (162), 17-24, 1993.

[53] Hall, C., "Water Sorptivity of Mortars and Concretes: A Review," Magazine of Concrete Research, **41** (147), 51-61, 1989.

[54] Dhir, R.K., Hewlett, P.C., and Chan, Y.N., "Near-Surface Characteristics of Concrete: Assessment and Development of In Situ Test Methods," Magazine of Concrete Research, **39** (141), 183-195, 1987.

[55] Blight, G.E., and Lampacher, B.J., "Applying Covercrete Absorption Test to In-Situ Tests on Structures," Journal of Materials in Civil Engineering, **7** (1), 1-8, 1995.

[56] Noble, A.E., Miller, E.R., and Derbyshire, H., "An Automated Method for the Measurement of Surface Water Absorption into Permeable Materials," Construction and Building Materials, **9** (1), 3-11, 1995.

[57] Basheer, P.A.M., Montgomery, F.R., and Long, A.E., "**CLAM** Tests for Measuring In-Situ Permeation Properties of Concrete," Nondestructive Testing and Evaluation, **12**, 53-73, 1995.

[58] Dhir, R.K., Shaaban, I.G., Claisse, P.A., and Byars, E.A., "Preconditioning In Situ Concrete for Permeation Testing Part I: Initial Surface Absorption," Magazine of Concrete Research, **45** (163), 113-118, 1993.

[59] Nolan, E., "Influence of Near Surface Moisture Gradients in Concrete on Autoclam Permeation Measurements," Ph. D. Thesis, The Queen's University of Belfast, 1996.

[60] Figg, J.W., "Methods for Measuring the Air and Water Permeability of Concrete," Magazine of Concrete Research, **25** (85), 213-219, 1973.

[61] Figg, J., "Concrete Surface Permeability: Measurement and Meaning," Chemistry and Industry, 714-719, 1989.

[62] Cather, R., Figg, J.W., Marsden, A.F., and O'Brien, T.P., "Improvements to the Figg Method for Determining the Air Permeability of Concrete," Magazine of Concrete Research, **36** (129), 241-245, 1984.

[63] Parrott, L., and Hong, C.Z., "Some Factors Influencing Air Permeation Measurements in Cover Concrete," Materials and Structures, **24**, 403-408, 1991.

[64] Lydon, F.D., and Odaallah, M. Al, "On-Surface Relative Permeability Test for Concrete," Construction and Building Materials, **2** (2), 1988.

[65] Torrent, R.J., "A Two-Chamber Vacuum Cell for Measuring the Coefficient of Permeability to Air of the Concrete Cover on Site," Materials and Structures, **25**, 358-365, 1992.

[66] Whiting, D.A., and Cady, P.D., "Condition Evaluation of Concrete Bridges Relative to Reinforcement Corrosion Volume 7: Method for Field Measurement of Concrete Permeability," SHRP-S-329, 1993.

[67] http://www.wsdot.wa.gov/fossc/OTA/SHRP/evals/.

[68] "Standard Test Method for Determining the Relative Permeability of Concrete by Surface Air Flow," AASHTO TP26-94, 7 pages.

[69] Self-Desiccation and Its Importance in Concrete Technology, Ed. B. Persson and G. Fagerlund (Lund University. Lund. Sweden. 1997).

[70] Parrott, L.J., "Assessing Carbonation in Concrete Structures," Proceedings of the 5th International Conference on Durability of Building Materials and Components, Brighton, 575-586, 1990.

[71] Parrott, L.J., "Moisture Profiles in Drying Concrete," Advances in Cement Research, **1** (3), 164-170, 1988.

[72] Andrade, C., Sarria, J., and Alonso, C., "Relative Humidity in the Interior of a Concrete Exposed to Natural Weathering," Cement and Concrete Research, **29** (8), 1249-1259, 1999.

[73] Bentz, D.P., and Garboczi, E.J., "Computer Modelling of Interfacial Transition Zone Formation and Resultant Properties," in RILEM ETC REPORT (RILEM, Paris, France, 1999).

[74] Spencer, R.W., "Measurement of the Moisture Content of Concrete," Journal of the American Concrete Institute, **34**, 45-61, 1937.

[75] Hancox, N.L., "An Electrical Measurement of the Effective Cross-Sectional Area for Conduction or Flow Processes in Cement Paste," Magazine of Concrete Research, **20** (64), 171-176, 1968.

[76] Bracs, G., Balint, E., and Orchard, D.F., "Use of Electrical Resistance Probes in Tracing Moisture Permeation Through Concrete," ACI Journal, **67**, 642-645, 1970.

[77] Woelfl, G.A., and Lauer, K., "The Electrical Resistivity of Concrete with Emphasis on the Use of Electrical Resistance for Measuring Moisture Content," Cement, Concrete, and Aggregates, **1** (2), 64-67, 1979.

[78] Whittington, H.W., McCarter, J., and Forde, M.C., "The Conduction of Electricity Through Concrete," Magazine of Concrete Research, **33** (114), 48-60, 1981.

[79] McCarter, W.J., Emerson, M., and Ezirim, H., "Properties of Concrete in the Cover Zone: Developments in Monitoring Techniques," Magazine of Concrete Research, **47** (172), 243-251, 1995.

[80] McCarter, W.J., "Monitoring the Influence of Water and Ionic Ingress on Cover-Zone Concrete Subjected to Repeated Absorption," Cement, Concrete, and Aggregates, **18** (1), 55-63, 1996.

[81] Kropp, J., "Corrosion Mechanisms of Concrete and Their Relevant Transport Processes," in The Modelling of Microstructure and Its Potential for Studying Transport Properties and Durability, Eds. H.M. Jennings, K.L. Scrivener, and J. Kropp (Kluwer Academic Publishers, 1996) pp. 457-471.

[82] Parrott, L.J., "Carbonation, Moisture, and Empty Pores," Advances in Cement Research, **4** (15), 111-118, 1991/92.

[83] Parrott, L.J.,"Water Absorption in Cover Concrete," Materials and Structures, **25**, 284-292, 1992.

[84] Balayssac, J.P., Detriche, Ch.H., and Grandet, J., "Interet de l'essai d'absorption d'eau pour la caracterisation du beton d'enrobage," Materials and Structures, **26**, 226-230, 1993.

[85] Balayssac, J.P., Detriche, Ch.H., and Diafat, N., "Influence de la duree de cure humide sur les caracteristiques du beton de peau," Materials and Structures, **31**, 325-328, 1998.

[86] Parrott, L.J., "Design for Avoiding Damage Due to Carbonation-Induced Corrosion," in ACI SP-145 Durability of Concrete, Ed. V.M. Malhotra (ACI, Detroit, Michigan, 1994) pp. 283-298.

[87] Ballim, Y., and Lampacher, B.J., "Long-Term Carbonation of Concrete Structures in the Johannesburg Environment," J. SA Inst. Civ. Eng., **38** (1), 5-9, 1996.

[88] Atkinson, A., and Hearne, J.A., "Mechanistic Model for the Durability of Concrete Barriers Exposed to Sulphate-Bearing Groundwaters," MRS Symposium Proceedings, **176**, 149-156, 1990.

[89] McCarter, W.J., Ezirim, H., and Emerson, M., "Absorption of Water and Chloride Into Concrete," Magazine of Concrete Research, **44** (158), 31-37, 1992.

[90] Lagerblad, B., and Utkin, P., "Silica Granulates in Concrete - Dispersion and Durability Aspects," CBI Report 3:93, Swedish Cement and Concrete Research Institute, 1993.

[91] Nilsson, L.O., "The Relation Between the Compostion, Moisture Transport and Durability of Conventional and New Concretes," Concrete Technology: New Trends, Industrial Applications, Ed. A. Aguado, R. Gettu, and S. Shah (E & FN Spon, London, 1996) pp. 63-82.

[92] Capra, B., and Bournazel, J.P., "Modeling of Induced Mechanical Effects of Alkali-Aggregate Reactions," Cement and Concrete Research, **28** (2), 251-260, 1998.

[93] Annual Book of ASTM Standards, Vol. 4.02 Concrete (ASTM, West Conshohocken, PA, 1998).

[94] Bager.D.H., and Jacobsen, S., "A Model for the Destructive Mechanism in Concrete Caused by Freeze/Thaw Action," RILEM workshop on Frost Damage in Concrete, Minneapolis, 1999.

[95] Jacobsen, S., "Liquid Uptake Mechanisms in Wet Freeze/Thaw: Review and Modelling," RILEM workshop on Frost Damage in Concrete, Minneapolis, 1999.

[96] Bentz, D.P., Garboczi, E.J., and Snyder, K.A., "A Hard Core/Soft Shell Microstructural Model for Studying Percolation and Transport in Three-Dimensional Composite Media," NISTIR **6265**, U.S. Department of Commerce, 1999.

[97] Handbook of Chemistry and Physics, 63rd Ed. (CRC Press, Boca Raton, Florida, 1982) pp. F-35.

[98] Ho, D.W.S., and Lewis, R.K., "Research into Curing Techniques and Their Effectiveness - The Major Findings," Concrete in Australia, **18** (2), 3-7, 1992.

[99] "Recommendations of TC 116-PCD: Tests for Gas Permeability of Concrete C. Determination of the Capillary Absorption of Water of Hardened Concrete," Materials and Structures, **32** (217), 178-179, 1999.

[100] "Recommendations of TC 116-PCD: Tests for Gas Permeability of Concrete B. Measurement of the Gas Permeability of Concrete by the RILEM-CEMBUREAU Method," Materials and Structures, **32** (217), 176-178, 1999.

[101] Filliben, J.J., "DATAPLOT: Introduction and Overview," NBS Special Publication No. 667, U.S. Department of Commerce, Washington, D.C., 1984.

Appendix

A Example Calculation of Service Life of Concrete Exposed to Sulfate Attack

For the example calculation, we will use the following values taken from Atkinson and Hearne [88]:

E=20 * 10^9 N/m

v= 0.3

α=1

β= 1.8 * 10^{-6} m^3/mol

γ_f= 10 N/m

We will assume a simple weather exposure consisting of one rainfall per month, of a duration of 1 day (86400 s). For our penetration coefficient, we will use a value of 10 $mm/h^{0.5}$ [98] or 0.000167 $m/s^{0.5}$. This will result in a penetration depth during the one day rainfall of 0.049 m. Our failure criteria will be 0.0127 m (1/2 in) of spalled concrete. We will use a conversion factor of 0.5 moles ettringite per mole of external sulfate, assuming that 2 moles of sulfate are required for the conversion from monosulfoaluminate to ettringite. The external sulfate concentration will be 0.01 M (or 10 mol/m^3 solution). Considering a concrete of 10 % porosity, this corresponds to a concentration of 1 mol sulfate/m^3 of concrete. Since X_{spall} decreases as C_E increases, for the case of sorption, failure will first occur at the depth of maximum penetration, 0.049 m. Solving for C_E in Equation 19, we find:

$$C_E = \frac{1}{\beta}\sqrt{\frac{2\alpha\gamma_f(1-\nu)}{EX_{spall}}}. \tag{23}$$

Substituting in all the relevant values, we find that C_E is equal to 66 mol/m^3. With 12 rainfalls per year, the cumulative C_E buildup after t_y years is, via Equation 20:

$$C_E(t_y) = 0.5 \times (1\ mole/m^3\ concrete) \times 12 \times t_y. \tag{24}$$

With C_E equal to 66, we find that the service life is estimated as 11 years for this relatively severe exposure environment.

B Proposed Testing Guidelines

B.1 Pre-Conditioning

1. Scope

These guidelines describe a laboratory method for the pre-conditioning of cylindrical concrete specimens prior to evaluation of their transport properties. It is well established that the transport coefficients of concretes vary strongly with the moisture content and internal relative humidity of the specimen. The goal of this method is to provide a series of specimens of various spatially uniform moisture contents typical of field conditions. The method is applicable to concrete grades for pavement applications as well as for similar cement-based materials used in construction.

2. Pre-conditioning method

2.1 Specimen preparation

Concrete cores, either cast or obtained from field concrete, are first sawn to obtain the thickness required for assessment of transport properties (see sections B.2 and B.3). The mass of each slice is determined and each slice is labelled with respect to its position in the original cylinder (e.g., outer surface, innermost surface, etc.). In order to avoid a moisture exchange of the test specimen with the ambient air during the absorption experiment and to assure that subsequent drying is one-dimensional, the free surfaces shall be sealed against the penetration of water vapor. The circumferential or vertical surfaces of the test specimens should be sealed using one of the following materials: self adhesive tape, epoxy adhesive paint, or paraffin. The mass of the specimen before, M_0, and after, M_a, the application, of the seal is recorded. To increase the reproducibility of the pre-conditioning, the specimens are first conditioned to a known "initial" state. To do this, they are vacuum saturated in a solution of lime water (to avoid leaching of calcium hydroxide from the concrete). After vacuum saturation, the mass of each slice is recorded once more.

2.2 Pre-conditioning

The goal of the pre-conditioning is to obtain a uniform moisture distribution within the specimen in a fairly rapid manner. To do this, drying is accelerated by placing the specimens in an environmental chamber with a temperature of 50 °C and a relative humidity of about 80 %. Individual specimens are dried in this environment for either 1 d, 2 d or 4 d. (The times of 1 d, 2 d, and 4 d are somewhat arbitrary and may be revised as the laboratory research progresses). For each concrete, this will provide specimens with three different moisture contents, whose transport properties can be subsequently evaluated. After the initial drying period, the specimens are placed in sealed plastic bags and remain in the oven until a total pre-conditioning period of 7 d is reached. This "sealed bag" drying allows the moisture within the specimen to redistribute spatially, hopefully producing a uniform moisture distribution. It should be noted that this uniform moisture distribution is much more important for subsequent permeability measurements (where the entire sample thickness influences the measurement) than for sorptivity (where mainly the surface of the sample infuences the initial uptake of water).

After the 7 d of oven drying/water redistribution, the mass of each specimen is determined and its "internal" relative humidity is assessed by placing the specimen in a sealed plastic jar

and monitoring the relative humidity of the surrounding air. The plastic jar is placed in an environment with a temperature of (20±2) °C. Because of the large moisture content of the sample relative to the capacity of the surrounding air in the jar, the equilibrium RH of the air will be very close to that of the specimen. This equilibrium RH should be approached within approximately two days time.

3. Pre-conditioning report

The pre-conditioning report shall contain all available information on the characteristics of the conditioned concrete, in particular

- date of test and age of concrete
- identification of the test specimens
- description of concrete; type of cement, mixture proportions, aggregate grading
- curing method and duration
- dimensions of the specimens
- initial mass of each specimen (both before, M_0, and after, M_a, sealing it)
- mass of each specimen after vacuum saturation, M_{vs}
- length of drying period before sealing specimen in a plastic bag
- mass of the specimen after pre-conditioning, M_{pc}
- internal RH of the specimen after pre-conditioning

After the evaluation of transport properties, the specimen is typically dried at 105 °C. Based on the mass of the specimen after drying, (M_D), and the mass following vacuum saturation, the moisture content and saturation of the tested specimen may be readily determined and reported. For example, the total moisture content, θ, of the specimen is given by:

$$\theta = \frac{M_{vs} - M_D}{M_D - (M_a - M_0)} \tag{25}$$

where the moisture content is given in kg H_2O/kg dry concrete. Similarly, the saturation, ξ, after a specific pre-conditioning is given by:

$$\xi = \frac{M_{pc} - M_D}{M_{vs} - M_D}. \tag{26}$$

B.2 Sorptivity

1. Scope

These guidelines describe a laboratory method for the experimental determination of the water take-up of hardened concrete by capillary absorption on concrete specimens. The method is applicable to concrete grades for pavement applications as well as for similar cement-based materials used in construction. These guidelines were modelled after those published by RILEM TC 116-PCD on "Permeability of Concrete as a Criterion of its Durability" [99].

2. Test specimens

2.1 Size and shape of test specimens

The preferred shape of the test specimens will be a cylinder with a minimal thickness of 35 mm. Specimens with rectangular cross-section may be used if necessary but they might be harder to seal (see 4.1). It is recommended that at least three specimens shall be used for each test. If the specimens are sawn from one cylinder, their position relative to the original cylinder should be recorded. This information will allow the assessment of inhomogeneity in the cylinder.

2.2 Manufacturing of specimens

Specimens could be cored or cast specimens. The cored specimens need to be sawn in order to have at least one surface that is flat.

Cast specimens shall be manufactured in molds made of steel or polymer of sufficient rigidity and appropriate size. Pouring and compaction of the concrete shall comply with national regulations on the production of test specimens. No form oil or releasing agents shall be used on the bottom side of the mold when casting the specimens. If steel molds are used a separation of the hardened concrete from the mold is provided by covering the bottom of the mold with polyethylene sheets or films. If a release agent was used to cast the specimen, a thin layer of the bottom of the specimen needs to be sawn and discarded. During the first 24 h after pouring, the specimens are kept under wet burlap and a plastic sheet at an ambient temperature of (20 +/-2) °C. Then, the specimens are demolded and cured as specified. For a comparison of different concretes, the same curing procedures must be applied to each.

3. Preconditioning

After completion of the specified curing regime the specimens are preconditioned according to the guidelines in section B.1.

4. Test Method

4.1 Preparation of the test specimens

The circumferential or vertical surfaces of the specimen must be sealed as described in section B.1.

The top surface of the specimens shall be covered with an impermeable cover such as that used on the vertical surfaces. If the specimen will be used for other tests such as permeability measurements, a flexible and removable plastic should be used, such as a plastic bag held in place by a rubber band. This procedure is not usable for a specimen with a rectangular cross-section due to the difficulty in sealing the plastic bag at the sharp corners. Again the mass of the specimen after the application of the top cover, M_c, is recorded.

4.2 Test procedure

The capillary absorption test is carried out in the following steps:

- The test specimens and the water reservoir are in equilibrium with an ambient temperature of (20 +/-1) °C.
- The dimensions of the test specimens, in particular those describing the test area, are measured with an accuracy of 0.1 mm. The specimen bottom exposed surface area, A, is calculated and recorded.

- The mass of the prepared specimen, M_i, is measured immediately before testing to an accuracy of 0.01 g. This mass includes the sealant for the vertical surfaces and the top surface.
- The bottom side of the specimen is immersed in water (tap water) up to a maximum depth of 3 mm. The water level is kept constant during the duration of the test.
- The uptake of water by capillary absorption is measured through the mass of the specimen, $M(t)$, at time intervals of (1, 5, 10, 20, and 30) min, 1h, and then every hour up to 6 h. Twenty-four hours after the first contact with water the specimen mass needs to be recorded again.
- Before weighing, the surface in contact with water is pressed against a paper towel to remove any water excess.

Depending on the purpose of the test the duration of the suction period may be extended beyond 24 h, but is finished when the rising water front reaches the top surface or the slope of the mass gain versus time is constant.

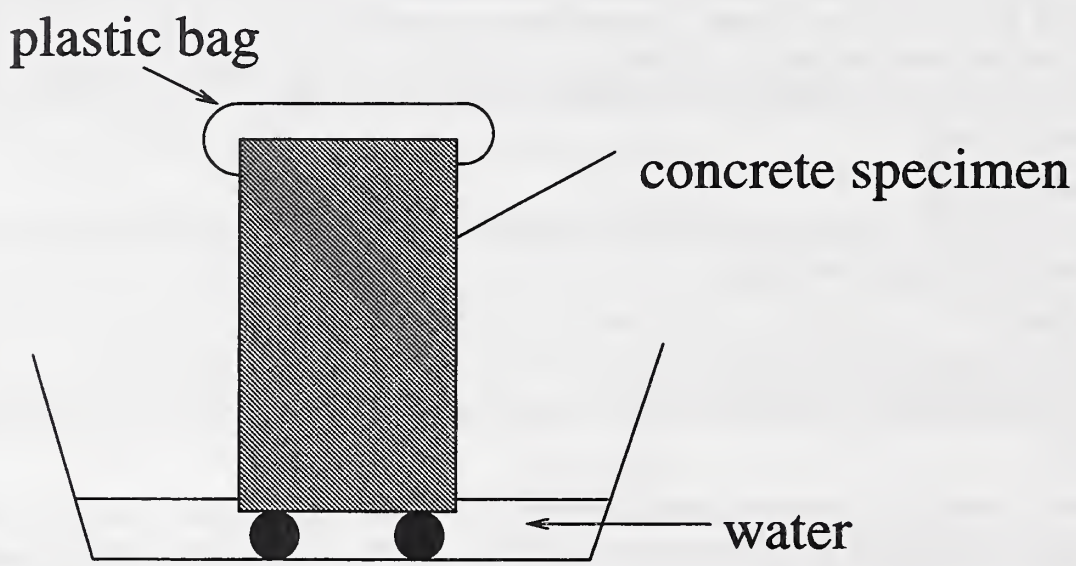

Figure 7: Basic NIST setup for laboratory evaluation of concrete sorptivity.

5. Calculation and presentation of the results

5.1 Evaluation of results

The water absorption per unit area, w_s, of each test specimen

$$w_s(t) = \frac{(M(t) - M_i)}{A} \tag{27}$$

is recorded and presented for each of the specified time intervals in [g/m^2]. Together with the absorption data the area of the tested surface is given for each specimen.

The data, $w_s(t)$, should be plotted versus time and the square root of time. The time at which the slope of $w_s(t)$ vs. $\sqrt{t}$ changes should be recorded. The points recorded before

the change of slope should be used to determine the sorptivity coefficient. The sorptivity coefficient is the slope of $w_s(t)$ vs. $\sqrt{t}$ without the initial point at t=0 (i.e., before contact with the water).

It also may be interesting for comparison purposes to determine the total intake of water per unit of mass, W. It can be calculated by the following equation:

$$W = \frac{M(t) - M_i}{M_0} \tag{28}$$

5.2 Test report

The test report shall include all available information on the characteristics of the tested concrete, in particular

- date of test and age of concrete
- identification of the test specimens
- description of concrete; type of cement, mixture proportions, aggregate grading
- curing method and duration
- preconditioning method and duration
- dimensions of the specimens
- mass of the specimen before and after sealing it
- test results: the mass of water absorption [g] and the water absorption per unit area of the test surface [g/m^2] for the respective suction periods
- sorptivity coefficient
- plots of the water absorption per unit area of the test surface vs. time and square root of time

B.3 Gas Permeability

1. Scope

The guidelines describe a laboratory method for the experimental detemination of the nitrogen permeability of a hardened concrete specimen. The method is applicable to concrete grades for pavement applications as well as for other cement-based materials used in construction. These guidelines are modelled after those published by RILEM TC 116-PCD on "Permeability of Concrete as a Criterion of its Durability" [100].

2. Test Specimens

2.1 Size and shape of test specimens

The test specimens are preferably cylinders 100 mm (4 in) in diameter and 37.5 mm in length. Alternatively, cylinders 75 mm (3 in) in diameter can be used in the same testing apparatus with minor modifications. It is recommended that at least three specimens be used for each test. If the specimens are sawn from a larger cylinder, their position relative to the original cylinder should be recorded (e.g., top surface, 2nd interior slice, etc.). This

information will allow the detection of inhomogeneity in the cylinder due to casting, improper consolidation, improper curing, etc.

2.2 Manufacturing of specimens

Specimens could be cored or cast specimens. The cored specimens need to be sawn in order to have at least one surface that is flat.

Cast specimens shall be manufactured in molds made of steel or polymer of sufficient rigidity and appropriate size. Pouring and compaction of the concrete shall comply with national regulations on the production of test specimens. No form oil or releasing agents shall be used on the bottom side of the mold when casting the specimens. If steel molds are used a separation of the hardened concrete from the mold is provided by covering the bottom of the mold with polyethylene sheets or films. If a release agent was used to cast the specimen, a thin layer of the bottom of the specimen needs to be sawn and discarded. During the first 24 h after pouring, the specimens are kept under wet burlap and a plastic sheet at an ambient temperature of (20 +/-2) °C. Then, the specimens are demolded and cured as specified. For a comparison of different concretes, the same curing procedures must be applied to each.

3. Preconditioning

After completion of the specified curing regime the specimens are preconditioned according to the guidelines provided in section B.1.

4. Test Method

4.1 Preparation of the test specimens

In order to assure one-dimensional flow during the permeability test, the sides of the cylindrical specimens should be sealed as outlined in section B.1. The bottom surface of the specimen is examined to ensure that it will provide a good seal against the silicone rubber spacing ring placed into the bottom the test specimen collar (see Figure 8).

4.2 Test procedure

The length of the test specimen is measured to the nearest 0.1 mm. This can be performed by measuring the length of the specimen at ten points equally spaced around the perimeter. Each measurement is performed to an accuracy of 0.1 mm, and the resulting average and standard deviation are reported. The specimen is sealed into the specimen frame using the screws around its circumference. Pressurized nitrogen gas is supplied at the inlet and the flowrate emanating from the top surface of the sample is monitored using either a bubble flowmeter or a digital flowmeter. Resolution of commonly available digital flowmeters are on the order of 0.1 ml/min, which limits the permeabilities which can be evaluated using this technique. A series of concentric o-rings divide the top surface into three monitoring areas (inner, middle, and outer) each with a slightly different area for flow. The areas of each of these flow areas are measured in advance. The initial seal of the specimen via the silicone rubber spacing ring can be rapidly evaluated by applying a pressure of 0.276 MPa (40 psia) and listening for leaks or monitoring the stability of the inlet pressure signal.

The measurements are carried out at inlet pressures above atmospheric varying from 0.069 MPa (10 psi) to 0.414 MPa (60 psi) in 0.069 MPa (10 psi) increments. At each pressure, the flowrates are monitored until they have equilibrated and then are recorded for each of the three monitoring sections.

5. Calculation and presentation of the results

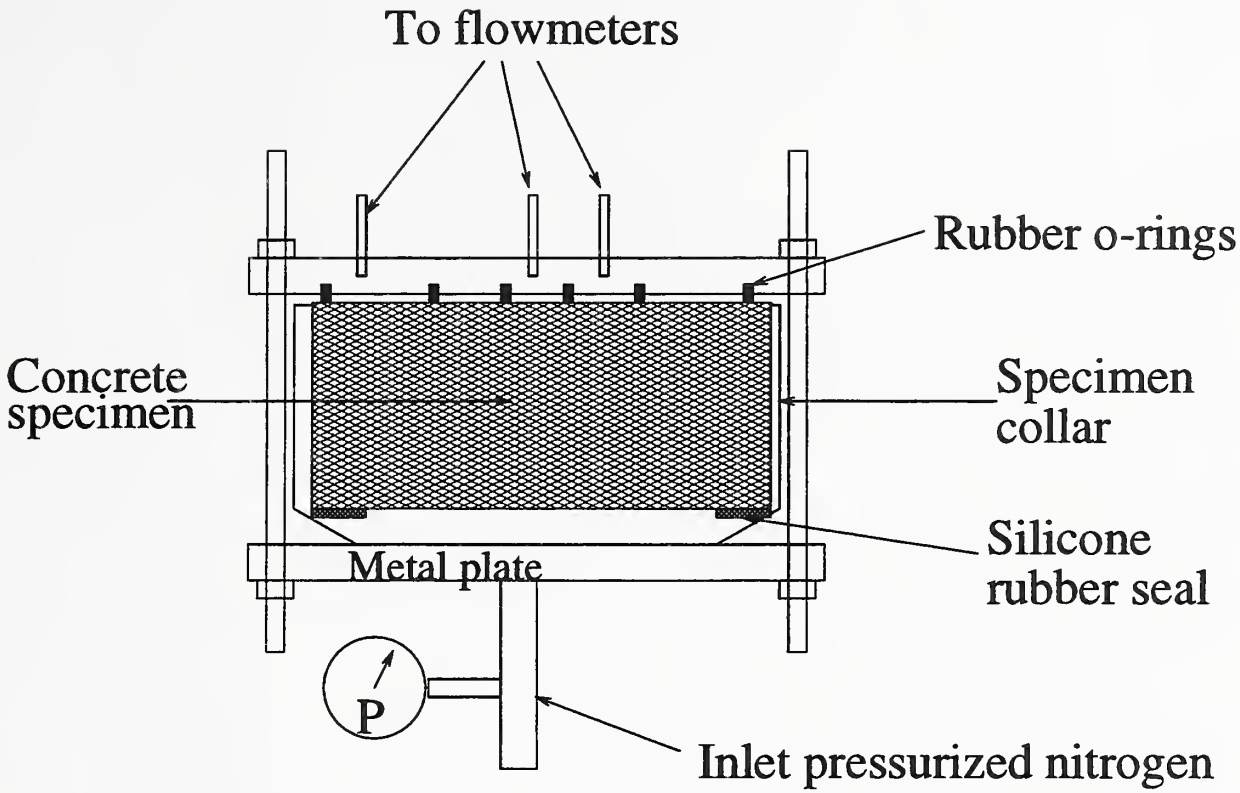

Figure 8: Basic NIST setup for laboratory evaluation of concrete gas permeability.

5.1 Results

The results obtained at different pressures are fit to Equations 8 and 9 to determine the intrinsic permeability, k_l for each monitoring section. A non-linear regression package, such as that provided by Dataplot [101], can be used to determine the "best" values of k_l for the flowrates measured at the different pressures. The computed values of k_l should be reported for each monitoring section.

5.2 Test report

The test report shall include all available information on the characteristics of the tested concrete, in particular

- date of test and age of concrete
- identification of the test specimens
- description of concrete; type of cement, mixture proportions, aggregate grading
- curing method and duration
- preconditioning method and duration
- dimensions of the specimens
- test results: measured flowrates for each pressure and each monitoring area for each specimen evaluated
- calculated intrinsic permeability coefficients